CHAPTER 4

A Mathematical Method for Designing a Set of Colour Scanning Filters

The goal of the colour scanning process has been defined in Chapter 3 as that of obtaining the s-stimulus values $\mathbf{V}^T\mathbf{f}$. In any multi-band image-recording problem of this sort, physical filters need to be designed and manufactured. In many instances the filters are to be chosen from a bank of existing filters. In other cases, the filters are to be manufactured. In either situation, the design procedure should incorporate the necessary constraints to obtain filters that are physically realizable, either from a set of existing filters, or through a manufacturing process. The combined effect of the optical path, the recording illuminant and the detector sensitivity, which must also be taken into account, often complicates the design procedure.

This chapter formulates the design of a set of three or more colour scanning filters as an optimization problem. The optimization criterion is the data-independent measure of goodness developed in Chapter 3. This criterion is different from those used by other researchers [5, 6, 9, 41] in that it measures the joint performance of the set of filters as a whole and not the performance of individual filters. Most of the literature in the design of colour scanning filters reports optimization routines that minimize a norm of the difference between each constructed filter and the corresponding vector in $\{\mathbf{La}_i\}_{i=1}^3$ [5, 9, 41], or maximize the q-factor (defined by Neugebauer [22]) of the individual scanning filters [6]. The measure defined in [7] is the average of the q-factors

of the individual filters and hence a measure of the individual filters. There has been no reported research on the use of a measure of the entire set of colour scanning filters as an optimization criterion.

In the case when the filters are to be chosen from a discrete set of filters, the problem may be solved by an exhaustive search. When the filters are to be fabricated, problems of physical realizability lead to a parametrized optimization problem which may be solved using existing optimization algorithms. The method described in this chapter has proved useful for colorimetric applications, as demonstrated in section 4.4. It can also be used for the design of filters for other multi-band image recording problems, specifically for the design of filters with applications in satellite imagery. The method proposed can be used for any scanning system for which the scanner characteristic (defined in section 2.7.8 as the combined effect of the lamps, light path and sensor characteristic) is known. Simulations and results from actual hardware demonstrate the utility of the method.

This chapter is organized as follows. Section 1 presents a method of choosing the 'best' set of colour scanning filters from an existing set of colour filters like the Kodak Wratten gelatin filters. Results from hardware implementations are presented. Section 2 presents the motivation behind posing the filter design problem as one of constrained optimization. Section 3 presents some ways of parametrizing the problem of designing a 'good' set of colour scanning filters when the filters are to be fabricated. Section 4 presents the implementation of the parametrizations of section 3 for particular scanner characteristics. The optimal values obtained, and the designed and fabricated filters, are reported. Section 5 presents a method of trimming the optimal filters of section 4 to get filters with optimal performance with respect to the average square ΔE_{Lab} error over a data set, and also with respect to the data-

independent measure of Chapter 3. The average square ΔE_{Lab} error over a data set can be used as an optimization criterion only for trimming because the implementation is too computationally expensive without smooth, close-to-optimal filters to start with, and because starting with smooth, close-to-optimal filters is one way of ensuring smoothness. Section 6 presents the use of projection methods to solve the optimization problem. Conclusions are presented in Section 7.

4.1 An Optimal Subset of a Discrete Set of Filters

The simplest formulation of the optimization problem occurs in the case when the 'best' set of r filters is to be chosen from a set of existing filters. Suppose the diagonal matrix **H** (see section 2.7.8), representing the combined effect of the optical path, the recording illuminant and the detector response, is known. Suppose the set S is the set of existing filters from which the best subset M_0 of r filters is to be chosen. Suppose **M** represents a subset of S, consisting of r filters. The matrix **HM** represents the effective set of scanning filters. The data-independent measure of this system, explicitly in terms of **M**, is, from equation (3.22):

$$\nu(\mathbf{V}, \mathbf{M}_H) \;=\; \frac{Trace\ (\mathbf{V}(\mathbf{V}^T\mathbf{V})^{-1}\mathbf{V}^T\mathbf{HM}(\mathbf{M}^T\mathbf{H}^T\mathbf{HM})^{-1}\mathbf{M}^T\mathbf{H}^T)}{\alpha} \tag{4.1}$$

if the matrices **HM** and **V** are assumed full-rank. The above expression for the measure may be optimized with respect to subsets of S, of size r, by an exhaustive search taking the filters r at a time, each filter representing a separate scanning filter. If n is the size of set S, such a search will involve ${}^nC_r \;=\; \frac{n!}{r!(n-r)!}$ evaluations of the measure, where ${}^nC_r$ represents the number of subsets of size r of a universal set of size n.

For example, given the set of Kodak Wratten filters, which are gelatin filters whose transmissivities are known, one can evaluate the measure for all possible combinations of r Wratten filters, given the matrices $\mathbf{H}$ and $\mathbf{V}$. The set with the highest value of the measure is the 'best' possible set of size r from the Wrattens for this particular application. The size of the Wratten filter set is approximately 100. This implies that the number of possible sets is $\frac{100!}{3!\ 97!}$ or approximately 1.6×10^5 to find the best set of three filters. It is much more computationally expensive to find the best set of 4 filters from the Wrattens, as this would involve computing the measure for approximately 4×10^6 filter sets.

Simulation results for an exhaustive search of the Wrattens to obtain the 'best' set of 3 filters for $\mathbf{V} = \mathbf{A}$, i.e. to determine the CIE tristimulus values under a uniform illuminant, are tabulated below. An actual scanner characteristic, Illuminant 1, shown in Fig. 4.1, was used. The Wratten filter numbers for the optimal set and a couple of other 'good' sets, the value of the measure, $\nu(\mathbf{A}, \mathbf{M}_H)$, and the average ΔE_{Lab} error of the corrected measurements (see section 2.2 and equation 3.8) over a set of Munsell chips, E, are tabulated in Table 4.1. Filter Set 1 was installed in the

Table 4.1: Optimal Subsets of the Wratten Filter Set

Filter Set	Wratten Filter Nos.	Measure $\nu(\mathbf{A}, \mathbf{M}_H)$	E
1	23A, 48A, 52	0.9122	2.04
2	9, 23A, 48A	0.9114	1.91
3	9, 48A, 52	0.9028	2.11

scanner at the Imaging Concepts Laboratory, Eastman Kodak, Rochester, NY. The scanning system was then used to scan the Munsell Chip Set. The resulting average

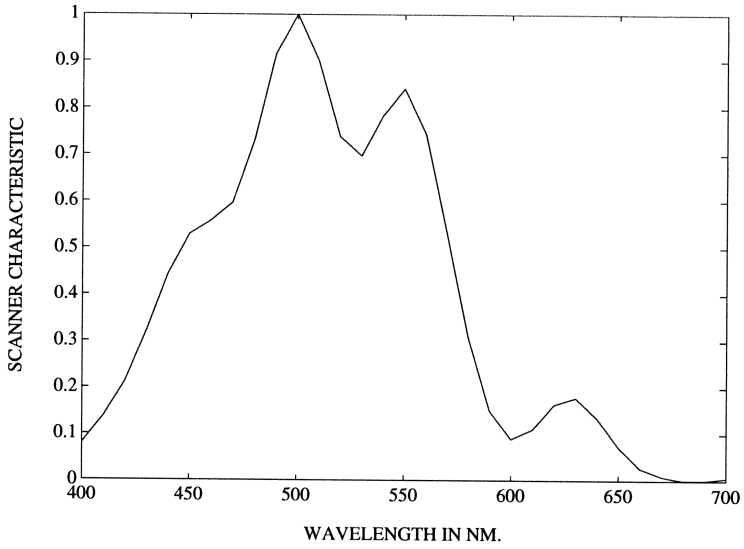

Figure 4.1: Illuminant 1

ΔE_{Lab} error of the corrected data was 3.02. The discrepancy may be attributed to several sources which are presently under investigation. The results obtained by the optimization should be compared to an average ΔE_{Lab} error of 4.5 obtained with the previously installed set designed by using the standard q-factor [15].

In particular cases the search can be simplified and some options discarded at the very beginning. In the above example, the Wrattens may be divided into three sets, and the filters chosen one from each set. This ensures that, for example, a set of three red filters is not considered in the search. Such assumptions result in reduction of the complexity of the search algorithm, but are very case-specific. In general, though, an exhaustive search where r << n will have a complexity $O(n^r)$.

In addition to the above-mentioned case of choosing three filters from a given set of filters, it is possible to construct a scanning filter by cascading more than one filter

from the given set of filters. The transmissivity of the resulting filter would be the product of the transmissivities of the individual filters, recall equation (2.8):

$$\mathbf{m} = \alpha \prod_{i=1}^{n} \mathbf{r}_i^{u_i}, \ for\ some\ \ \alpha,\ u_i \geq 0,$$

In an expression for a filter as the product of a number of existing filters, the density of each filter, u_i, may be treated as a variable. This makes the problem far more complex, and an exhaustive search of all such possibilities is much more computationally expensive. Reports exist in the literature of attempts to form scanning filters in such a manner [5, 9, 41]. Again, these attempts use a different optimization criterion as mentioned earlier.

4.2 An Unacceptable Solution to the Optimization Problem

Section 4.1 presents a method of choosing the best set of r scanning filters from an existing filter bank. When the filters are not to be chosen from a filter bank but are to be manufactured, there is much more freedom in the choice of filter characteristics, and it is expected that the measure of the optimal set will, in general, be larger than that of a set chosen from an existing filter bank. To take full advantage of the filter-manufacturing process, though, considerable attention must be paid to the limitations of the process of filter fabrication.

The expression for the data-independent measure in terms of the matrix $\mathbf{M}$ in equation (4.1) provides an optimization criterion for the design of filters that are to be manufactured. Notice that all matrices except the matrix $\mathbf{M}$ are known. The dimension of M is $N \times r$ where r is the number of scanning filters and N is the number of samples of a visible spectrum between 400 nm and 700 nm. In the examples

discussed here, N = 31. Without any other restrictions, the measure is a function of rN parameters, each parameter being the transmissivity of a filter at a particular wavelength. The filter design problem may be interpreted as an optimization problem where the goal is maximization of the measure with respect to each of the rN parameters.

A simple and straightforward solution to the optimization problem is

$$\mathbf{m}_i(k) = \kappa_i \frac{\mathbf{v}_i(k)}{\mathbf{h}(k)} \qquad i = 1,\ 2,\ 3, ...s; \quad \mathbf{h}(k) \neq 0 \tag{4.2}$$

where

$$\kappa_i = (\overset{max}{k}\ (\frac{\mathbf{v}_i(k)}{\mathbf{h}(k)}))^{-1} \tag{4.3}$$

is the normalization constant for the i^{th} filter so that the maximum transmissivity of each designed scanning filter is unity. Recall that $\mathbf{h}(k)$ represents the scanner characteristic at the k^{th} wavelength, and $\{\mathbf{v}_i\}_{i=1}^{s}$ represents the space to be spanned. The set of optimal filters of equation (4.2) consists of r filters such that $\mathbf{M}_H = \mathbf{V}\mathbf{\Lambda}_\kappa$ where $\mathbf{\Lambda}_\kappa$ is a diagonal matrix with diagonal values κ_i. The scanning system will replicate the vectors $\mathbf{v}_i$.

For the scanner characteristic of Fig. 4.1, and $\mathbf{V} = \mathbf{A}$, the three scanning filters defined by equation (4.2) are shown in Fig. 4.2. Notice that the scanner characteristic is far from uniform, with a very large dynamic range, and that this is likely to present problems in filter design. The filters designed according to equation (4.2) have a large dynamic range (of the order of 10^4), because of the large variation in values of $\mathbf{h}$(k). The large dynamic range is not by itself necessarily a problem, but the fact that low values of the designed filters may be associated with high values of the scanner characteristic could lead to problems. In particular, this leads to an ill-conditioned

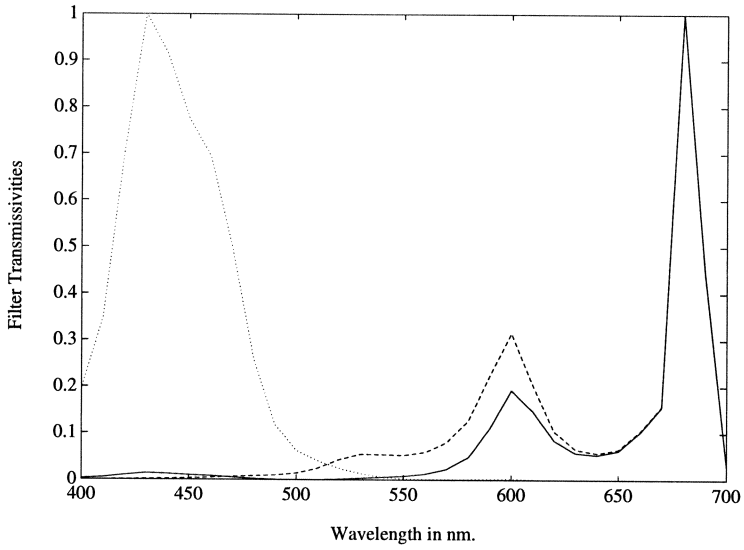

Figure 4.2: Filters for the Replication of the CIE Matching Functions with Scanner Characteristic 1

problem and high susceptability to small errors in the fabrication process. Further, smoothness of filter transmissivity curves is an important restriction in the filter fabrication process, and Fig. 4.2 indicates that filters designed according to equation (4.2) will not be easy to fabricate exactly. Another example of non-smooth filters of the form of equation (4.2) is presented in Fig. 4.4, which are CIE replications with another actual scanner characteristic, Illuminant 2, plotted in Fig. 4.3. This makes it clear that each constructable filter does not possess N degrees of freedom and that expressing the measure as a function of rN independent variables will not necessarily result in optimal *realizable* filters. The above example implies that the optimization problem should be formulated so that a non-smooth curve with a high dynamic range is not an acceptable solution to the problem of filter design.

To see the effect of fabrication errors on the performance of the filters, consider

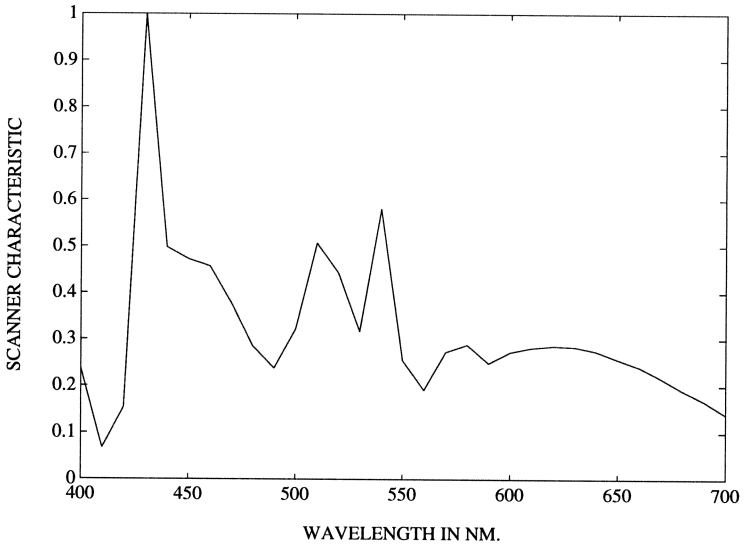

Figure 4.3: Illuminant 2

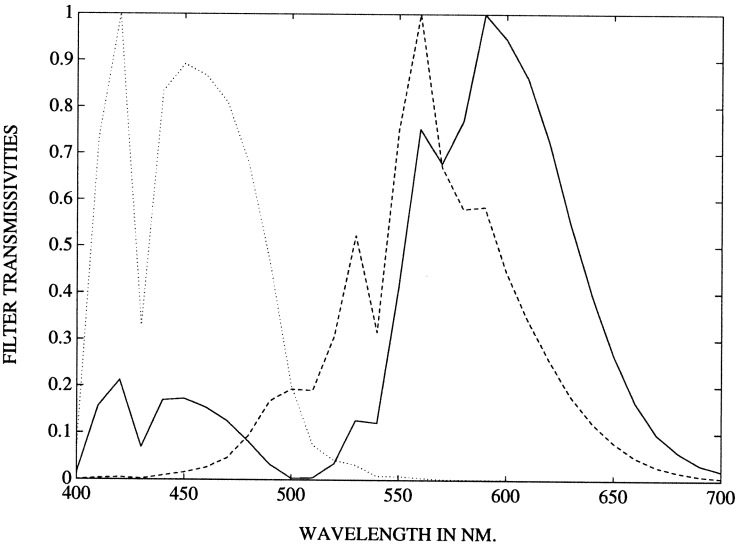

Figure 4.4: Filters for the Replication of the CIE Matching Functions with Scanner Characteristic 2

a transmissivity less than 0.01 at the k^{th} wavelength for a filter designed according to equation (4.2). A fabrication error of 0.01 can result in zero transmissivity at the corresponding point in the fabricated filter. The corresponding error in the effective scanning filter $\mathbf{Hm}_i$ at the k^{th} point is $\mathbf{h}(k)\mathbf{m}_i(k)$. This error is small if the corresponding value of $\mathbf{h}$(k) is small. If the fabrication error occurs at a wavelength where the scanner characteristic does not have a low value, then the fabrication error results in a considerably higher error in the resulting scanning system. For a quantitative analysis, consider the following. Suppose that

$$\mathbf{m}_{i_0}(k_0) \;=\; \kappa_{i_0}\frac{\mathbf{v}_{i_0}(k_0)}{\mathbf{h}(k_0)} \leq 0.01 \; for \; some \; i_0 \; and \; k_0 \tag{4.4}$$

An error of 0.01 in the fabrication process results in a value of zero for $\mathbf{m}_{i_0}(k_0)$, which in turn results in a value of zero for $\mathbf{Hm}_{i_0}(k_0)$, which results in an error of $\kappa_{i_0}\mathbf{v}_{i_0}$ in the effective scanning filter $\mathbf{Hm}_{i_0}$ at wavelength λ_{k_0}. A normalized value of this error is

$$\frac{\kappa_{i_0}\mathbf{v}_{i_0}(k_0)}{\underset{k}{max}\;\kappa_{i_0}\mathbf{v}_{i_0}(k)} \;=\; \frac{\mathbf{v}_{i_0}(k_0)}{\underset{k}{max}\;\mathbf{v}_{i_0}(k)}$$

To obtain an expression for the normalized error implied by inequality (4.4), consider the following. Equations (4.3) and (4.4) imply that

$$(\underset{k}{max}\;(\frac{\mathbf{v}_{i_0}(k)}{\mathbf{h}(k)}))^{-1}\frac{\mathbf{v}_{i_0}(k_0)}{\mathbf{h}(k_0)} \leq 0.01$$

The above inequality implies that

$$\frac{\mathbf{v}_{i_0}(k_0)}{\mathbf{h}(k_0)} \leq 0.01\;\underset{k}{max}\;(\frac{\mathbf{v}_{i_0}(k)}{\mathbf{h}(k)}) \leq 0.01\frac{\underset{k}{max}\;\mathbf{v}_{i_0}(k)}{\underset{k}{min}\;\mathbf{h}(k)}$$

which implies that

$$\frac{\mathbf{v}_{i_0}(k0)}{\underset{k}{max}\ \mathbf{v}_{i_0}(k)} \leq 0.01 \frac{\mathbf{h}(k_0)}{\underset{k}{min}\ \mathbf{h}(k)}$$

The above inequality provides an upper bound on the normalized error in terms of the dynamic range of the sensor characteristic:

$$\frac{\mathbf{v}_{i_0}(k0)}{\underset{k}{max}\ \mathbf{v}_{i_0}(k)} \leq 0.01 \frac{\underset{k}{max}\ \mathbf{h}(k)}{\underset{k}{min}\ \mathbf{h}(k)}$$

For the scanning filters of Fig 4.2,

$$\frac{\underset{k}{max}\ \mathbf{h}(k)}{\underset{k}{min}\ \mathbf{h}(k)} = 1314.4$$

which implies that normalized errors of approximately 13.14 are possible in the replications. As the defined normalized error cannot exceed unity, this implies that large normalized errors are possible. For the scanning filters of Fig. 4.4,

$$\frac{\underset{k}{max}\ \mathbf{h}(k)}{\underset{k}{min}\ \mathbf{h}(k)} = 14.837$$

and a maximum normalized error of approximately 0.1484 can occur.

The above calculations indicate that replications made with scanner characteristic 2 are less likely than those made with characteristic 1 to present the problems of amplification of fabrication error due to large dynamic range. The bound on the dynamic range of these filters is also smaller than the bound on the range for the filters designed using scanner characteristic 1. The large dynamic range is just one reason for the inadequacy of the design method. Another reason is non-smooth filters

resulting from non-smooth scanner characteristics. Equation (4.2) indicates that the designed filters will be highly non-smooth if the scanner characteristic is non-smooth because the CIE matching functions are fairly smooth. The effect of the non-smooth nature of the scanner characteristic is enhanced by the division of the values of $\mathbf{v}_i$ by the scanner characteristic, especially when the scanner characteristic takes on small values.

4.3 Parametrization of Filter Characteristics

One way of incorporating a manageable dynamic range and smoothness of the filters into the optimization algorithm is by modelling each filter in terms of known, smooth, non-negative mathematical functions. This section deals with the modelling of the filters as single gaussians, as the sum of two gaussians, as raised cosines and sums of raised cosines, and as exponential cosines. The modelling results in the parametrization of the filters in terms of the parameters defining the respective functions. The total number of parameters is less than 5r in each case, resulting in tractable formulations of the optimization problem and in physically realizable filters.

Parametrization of the filters implies parametrizing the measure as well. The measure is a function of at most 5r variables. The functional form of the measure in terms of the parameters is not simple, and it is not possible to find a closed-form solution to the resulting optimization problem. Various existing optimization algorithms may be used to find local points of extrema of the measure with respect to the parameters. It is not, in general, possible to find global extrema for functions such as the measure. However, it is possible to obtain a number of local points of extrema and present the optimal one among these as the optimal point. In general,

the local point of extremum obtained depends on the initial point.

4.3.1 Gaussian Filter Models

A gaussian function with mean μ and standard deviation σ is:

$$p(x) = \frac{1}{\sqrt{2\pi}\sigma} exp(-\frac{(x - \mu)^2}{2\sigma^2})$$

If each filter $\mathbf{m}_i$ is modelled as a gaussian function of mean μ_i and standard deviation σ_i the normalized filter vectors $\mathbf{m}_i$ are

$$\mathbf{m}_i(k) = exp(-\frac{(\lambda_k - \mu_i)^2}{2\sigma_i^2}) \tag{4.5}$$

where λ_k depends on the sampling of the spectra. Each filter is a function of 2 independent variables and the measure is a function of 2r independent variables. The resulting 'optimal' filters will be gaussians and hence easier to fabricate. The results for the single-gaussian filter model and the scanner characteristics in Figs. 4.1 and 4.3 are presented in Section 4.4. While the smaller number of parameters makes finding the optimal values mathematically tractable, the resulting filters have limited spectral shapes. Given the scanner characteristic, considerable flexibility in shape is required for 'good' filters. The results demonstrate that the single-gaussian model does not produce very good filters.

One way of allowing more freedom in filter design is to extend the single-gaussian model to a sum-of-gaussians model. Each filter may be modelled as the weighted sum of two gaussians. Each filter is then a function of 5 parameters (2 means, 2 variances and 1 weighting factor). This results in vectors $\mathbf{m}_i$ of the form

$$\mathbf{m}_i(k) = exp(-\frac{(\lambda_k - \mu_{i1})^2}{2\sigma_{i1}^2}) + \alpha_i exp(-\frac{(\lambda_k - \mu_{i2})^2}{2\sigma_{i2}^2}) \tag{4.6}$$

The function $\nu(\mathbf{A}_L, \mathbf{M}_H)$ is now a function of 5r variables. Standard optimization routines can provide values of the 5r parameters such that the measure is maximum, or close to maximum. Thus, one can find an optimal set of filters for particular scanner characteristics such that each filter is modelled as the sum of two gaussians. Section 4.4 presents the results obtained for the scanner characteristics of Figs. 4.1 and 4.3.

4.3.2 Raised-Cosine Filter Models

One cycle of the raised cosine function with period T and phase ζ is:

$$p(x, T, \zeta) = \begin{cases} (1 + cos(\frac{2\pi}{T}(x - \zeta)))/2 & |x - \zeta| \leq \frac{T}{2} \\ 0 & \text{else} \end{cases}$$

If each filter $\mathbf{m}_i$ is modelled as one cycle of a raised cosine function of period T_i and phase ζ_i, the filter vectors are:

$$\mathbf{m}_i(k) = \begin{cases} (1 + cos(\frac{2\pi}{T_i}(\lambda_k - \zeta_i)))/2 & |\lambda_k - \zeta| \leq \frac{T}{2} \\ 0 & \text{else} \end{cases} \tag{4.7}$$

or,

$$\mathbf{m}_i(k) = p(\lambda_k, T_i, \zeta_i)$$

Each filter is a function of 2 variables and the measure is a function of 2r variables.

The filters may also be modelled as weighted sums of one cycle each of raised cosines, so that

$$\mathbf{m}_i(k) = p(\lambda_k, T_{i1}, \zeta_{i1}) + \alpha_i p(\lambda_k, T_{i2}, \zeta_{i2}) \tag{4.8}$$

Each filter is a function of 5 variables and the measure is a function of 5r variables. Simulation results using raised-cosine filter models are presented in section 4.4.

4.3.3 Exponential-Cosine Filter Model

Another filter model is

$$\mathbf{m}_i(k) = \begin{cases} (exp(a_i cos(2\pi \frac{\lambda_k - \zeta_i}{T_i})) - exp(-a_i))/c_i & |\lambda_k - \zeta| \leq \frac{T}{2} \\ 0 & \text{else} \end{cases} \tag{4.9}$$

where $c_i = exp(a_i) - exp(-a_i)$ is a normalizing constant for the i^{th} filter. Each filter is a function of 3 variables, and the measure a function of 3r variables. Simulation results are presented in section 4.4.

In general, an increase in the number of parameters used to define the filters should give better results. An increase in the number of parameters, does, in general, increase computation time and also results in filters with more local maxima. In some instances, an increase in model parameters does not improve the set of filters substantially. To illustrate this, optimum sets with a sum-of-three-gaussians model are presented in section 4.4.

4.4 Experimental Results

For the particular scanner characteristics of Figs. 4.1 and 4.3, the parametrizations suggested in section 4.3 were implemented to obtain the 'best' set of colour scanning filters. The viewing illuminant was assumed uniform, i.e. $\mathbf{L} = \mathbf{I}$. From the results in this section it is clear that the filters obtained are very good. To test the performance of the filters, the scanning process was simulated using a set of spectra of Munsell chips. The average and maximum ΔE_{Lab} errors were calculated for corrected data (see section 2.2 and equation(3.8)).

4.4.1 Optimization Algorithm

For all parametrizations the MATLAB [43] function 'fmins' was used to find optimal filters. This function is an implementation of the Nelder-Meade simplex algorithm. The algorithm is iterative. Given a function of n variables to be optimized, the value of the function is evaluated at selected n+1 points at each iteration, to decide the direction to move in for the next estimate. The function 'fmins' is best for finding minima of functions with five or fewer unknown parameters.

Very clearly, the measure does not have one global maximum, as, for example, the filters in a different order will give a different point in parameter space but the same value of the measure. It is also likely that the measure has many local maxima which are not global maxima. This implies that a stopping point is a function of the starting point and not necessarily a global extremum. To minimize this effect several different initial points were used. The resulting filters gave varying but similar results.

4.4.2 Single-Gaussian Model

The parameters for the single-gaussian model of equation(4.5) were calculated for the scanner characteristics shown in Figs. 4.1 and 4.3. The measure of the resulting optimal set of filters, ν, the means, μ_1, μ_2 and μ_3, the standard deviations, σ_1, σ_2, and σ_3, and the average and maximum ΔE_{Lab} errors E and E_{max} over the set of Munsell chips for corrected estimates are tabulated in Table 4.2 for each case.

The designed filters for Illuminant 1 are plotted in Fig. 4.5. Barr Associates, a filter manufacturer, provided an estimate of the closest filters they could manufacture given the specifications for Illuminant 2 above. This closest filter set had a measure of 0.9478, an average ΔE_{Lab} error of 0.86, and a maximum ΔE_{Lab} error of 2.5. The

Table 4.2: Parameters for Single Gaussian Model

Filter Set	Illuminant	ν	Filter No. 1	Filter No. 2	Filter No. 3	E	E_{max}
1	1	0.9556	$\mu_1 = 438.3$ $\sigma_1 = 26.4$	$\mu_2 = 548.0$ $\sigma_2 = 37.6$	$\mu_3 = 607.0$ $\sigma_3 = 19.1$	1.75	9.16
2	2	0.9485	$\mu_1 = 459.1$ $\sigma_1 = 22.0$	$\mu_2 = 557.7$ $\sigma_1 = 40.3$	$\mu_3 = 592.9$ $\sigma_1 = 35.8$	0.84	2.46

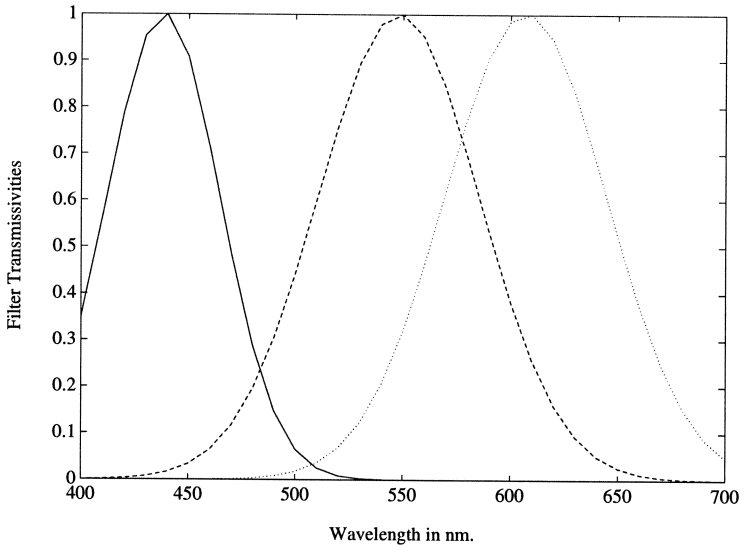

Figure 4.5: Designed Filters for Single-Gaussian Model and Illuminant 1

designed filters for Illuminant 2 and the closest filters Barr Associates can manufacture are shown as solid and dotted lines respectively in Figs. 4.6, 4.7 and 4.8.

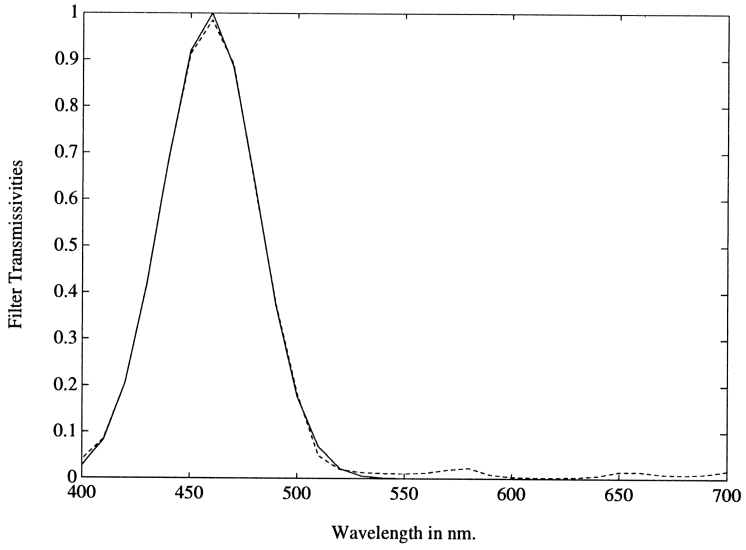

Figure 4.6: Designed and Fabricated (Blue) Filter for Single-Gaussian Model and Illuminant 2

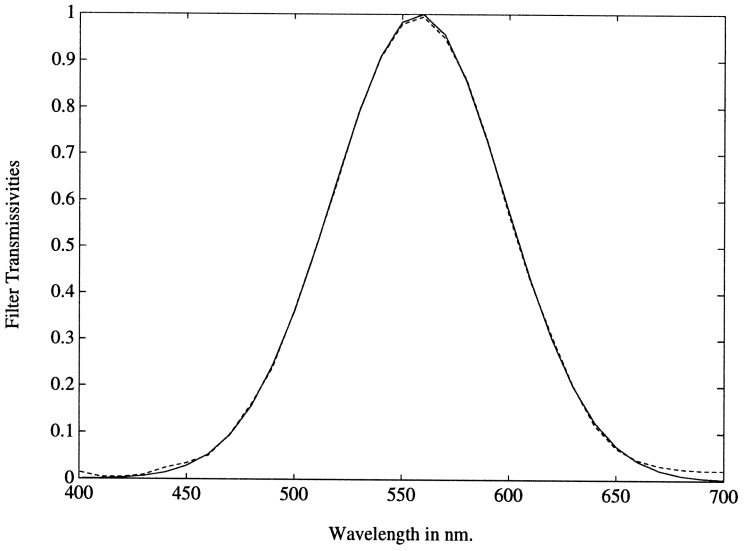

Figure 4.7: Designed and Fabricated (Green) Filter for Single-Gaussian Model and Illuminant 2

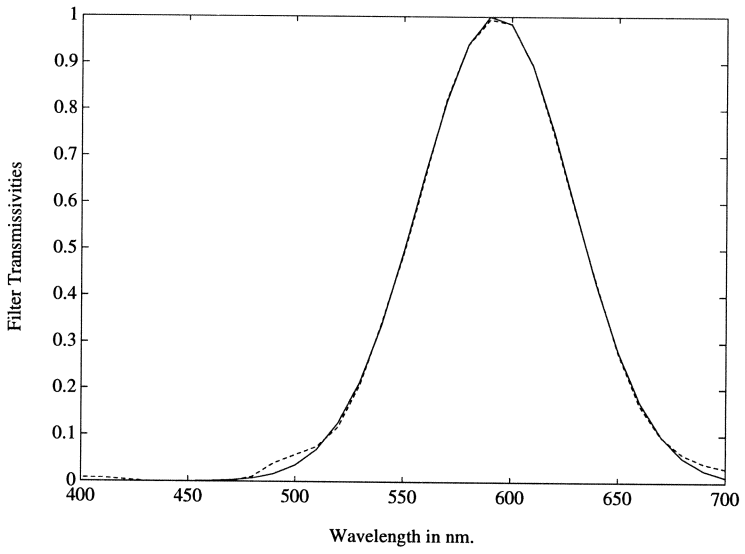

Figure 4.8: Designed and Fabricated (Red) Filter for Single-Gaussian Model and Illuminant 2

4.4.3 Sum-of-Gaussian Model

The parameter values obtained for the sum-of-gaussian filter model of equation (4.6) are tabulated in Table 4.3

Table 4.3: Parameters for Sum-of-Gaussian filter model

Filter Set	Illuminant	ν	Filter No. 1	Filter No. 2	Filter No. 3	E	E_{max}
1	1	0.9928	$\mu_{11} = 442.7$ $\sigma_{11} = 24.6$ $\mu_{12} = 428.2$ $\sigma_{12} = 7.0$ $\alpha_1 = 0.3022$	$\mu_{21} = 593.6$ $\sigma_{21} = 14.7$ $\mu_{22} = 539.9$ $\sigma_{22} = 29.0$ $\alpha_2 = 0.5281$	$\mu_{31} = 601.2$ $\sigma_{31} = 11.2$ $\mu_{32} = 638.1$ $\sigma_{32} = 49.4$ $\alpha_3 = 0.3969$	0.46	1.71
2	1	0.9832	$\mu_{11} = 116.8$ $\sigma_{11} = 7.1$ $\mu_{12} = 438.3$ $\sigma_{12} = 26.4$ $\alpha_1 = 1.1656$	$\mu_{21} = 545.3$ $\sigma_{21} = 0.6$ $\mu_{22} = 551.3$ $\sigma_{22} = 38.8$ $\alpha_2 = 0.0069$	$\mu_{31} = 642.8$ $\sigma_{31} = 57.2$ $\mu_{32} = 602.1$ $\sigma_{32} = 10.4$ $\alpha_3 = 2.2182$	1.25	7.45
3	2	0.9698	$\mu_{11} = 461.6$ $\sigma_{11} = 23.4$ $\mu_{12} = 443.7$ $\sigma_{12} = 4.1$ $\alpha_1 = 0.4558$	$\mu_{21} = 559.7$ $\sigma_{21} = 7.6$ $\mu_{22} = 549.3$ $\sigma_{22} = 43.8$ $\alpha_2 = 0.9552$	$\mu_{31} = 585.2$ $\sigma_{31} = 27.6$ $\mu_{32} = 622.0$ $\sigma_{32} = 25.5$ $\alpha_3 = 0.5897$	0.75	3.28

The designed filters of set 1 are plotted as solid lines and the filters of the set Barr Associates are able to manufacture are plotted as dotted lines in Figs. 4.9, 4.10 and 4.11. The measure of the filter set Barr Associates can manufacture with respect to the scanner it was designed for is 0.9900. The average ΔE_{Lab} error for the fabricated set was 0.50. The maximum ΔE_{Lab} error for the set was 1.95.

The designed filters of set 2 are plotted as solid lines and the filters of the set

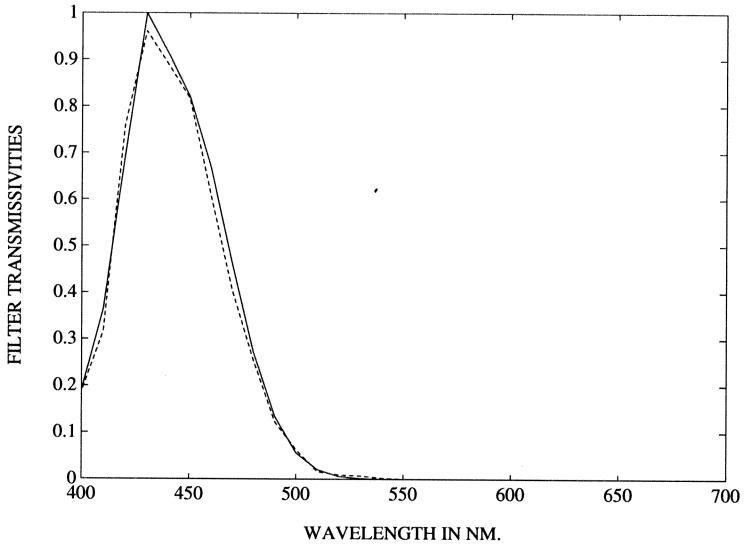

Figure 4.9: Designed and Fabricated (Blue) Filter for Double-Gaussian Model (Set 1) and Illuminant 1

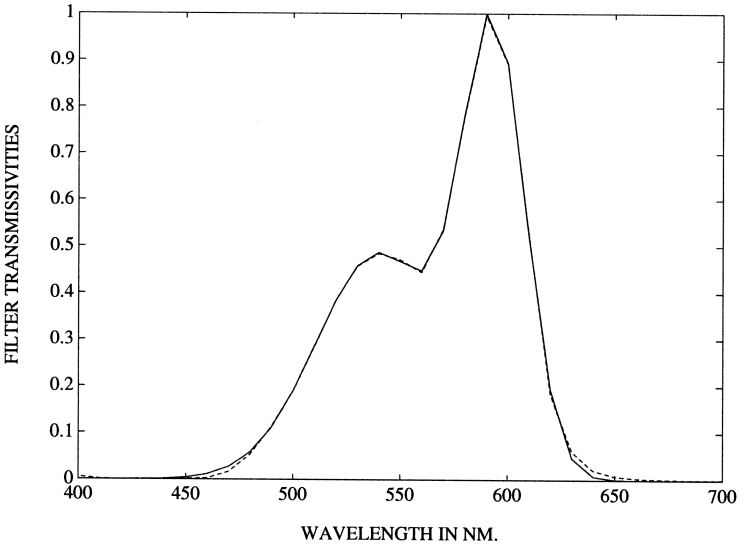

Figure 4.10: Designed and Fabricated (Green) Filter for Double-Gaussian Model (Set 1) and Illuminant 1

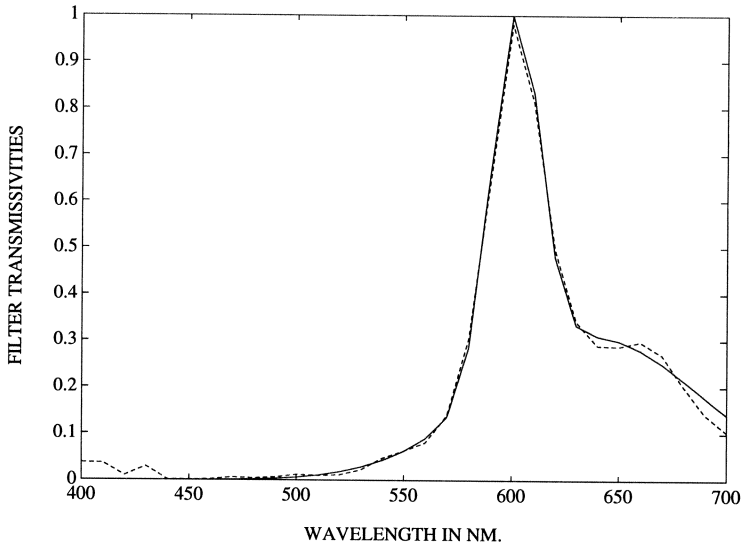

Figure 4.11: Designed and Fabricated (Red) Filter for Double-Gaussian Model (Set 1) and Illuminant 1

Eastman Kodak is able to manufacture are plotted as dotted lines in Figs. 4.12, 4.13 and 4.14. The measure of the set that can be manufactured is 0.9769, the average ΔE_{Lab} error is 1.10, and the maximum ΔE_{Lab} error is 6.94.

The two designs for scanner characteristic 1 were obtained from different initial points for the optimization algorithm. The filters that can be manufactured from both designs are sufficiently accurate as indicated by the errors in Table 4.3. Chapter 5 deals with the sensitivity of the data-independent measure and the mean square ΔE_{Lab} error to fabrication errors, and an analysis of the change in these values due to fabrication errors is presented there.

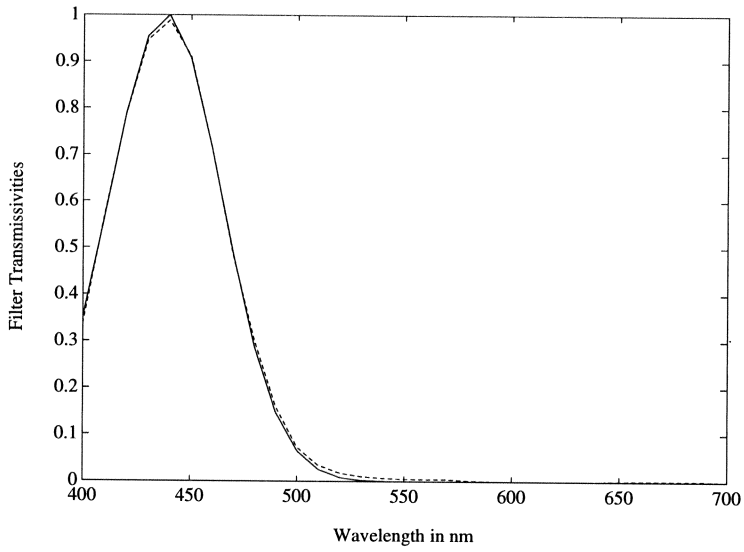

Figure 4.12: Designed and Fabricated (Blue) Filter for Double-Gaussian Model (Set 2) and Illuminant 1

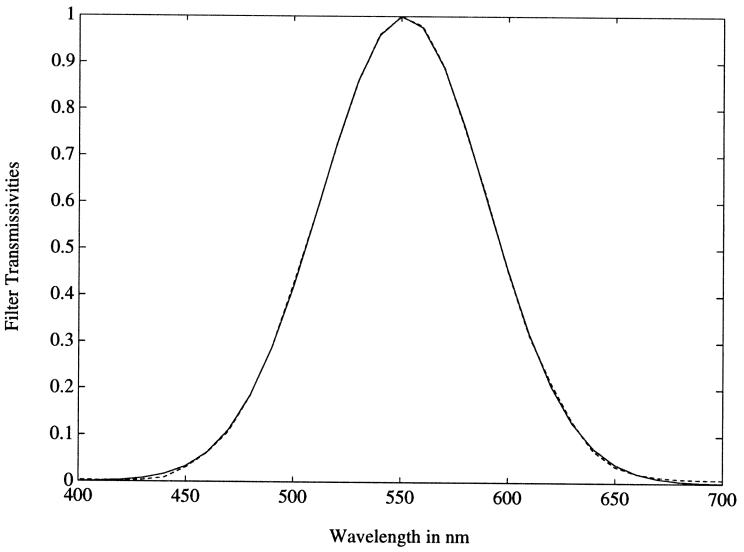

Figure 4.13: Designed and Fabricated (Green) Filter for Double-Gaussian Model (Set 2) and Illuminant 1

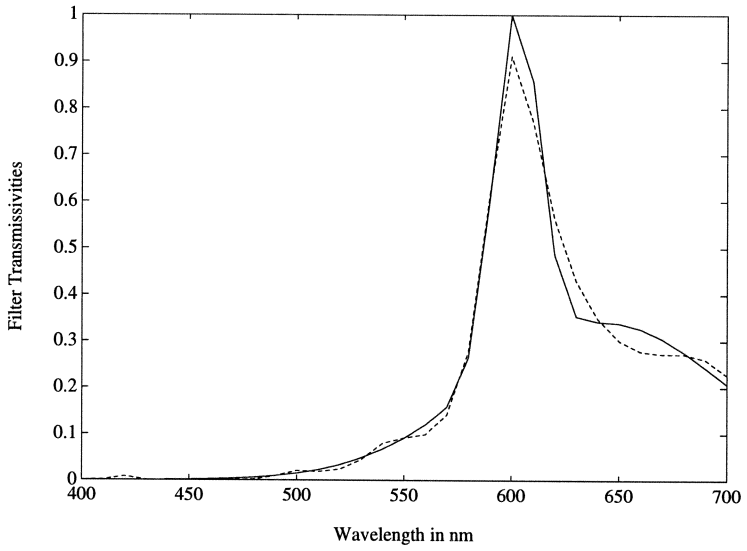

Figure 4.14: Designed and Fabricated (Red) Filter for Double-Gaussian Model (Set 2) and Illuminant 1

The designed filters for Set 3 are plotted in fig 4.15. The effective scanning filters

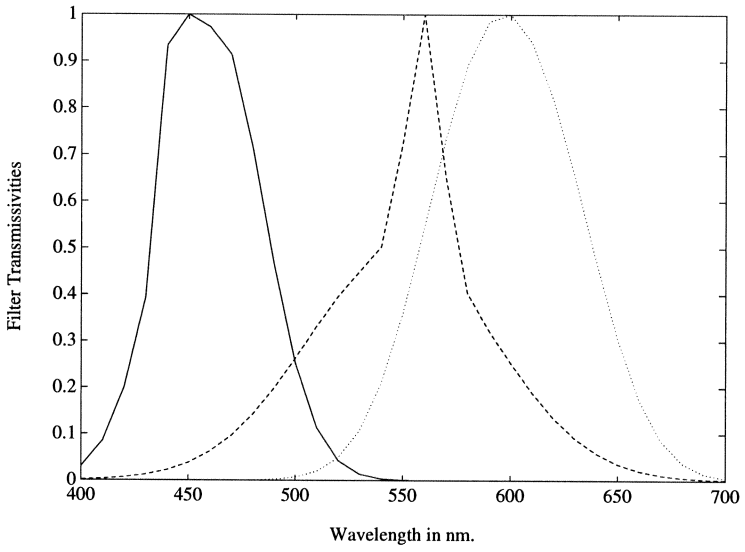

Figure 4.15: Designed Scanning Filters for Sum-of-Gaussian Model and Illuminant 2

of Set 3 i.e. the combined effect of the designed Filter Set 3 and Illuminant 2 are plotted in Fig. 4.16. These plots give an idea of what the combined effect of the scanning filters is, and illustrate that the effective filter set need not be 'close' to the CIE matching functions for a 'good' filter set.

4.4.4 Sum of Three Gaussians

Some experiments were performed to obtain the best sum-of-three-gaussians for the two illuminants. Using the optimal results for sum-of-two-gaussians presented in the previous section as intial estimates did not result in filters that were substantially different from the sum-of-gaussian ones. These results are hence not presented here.

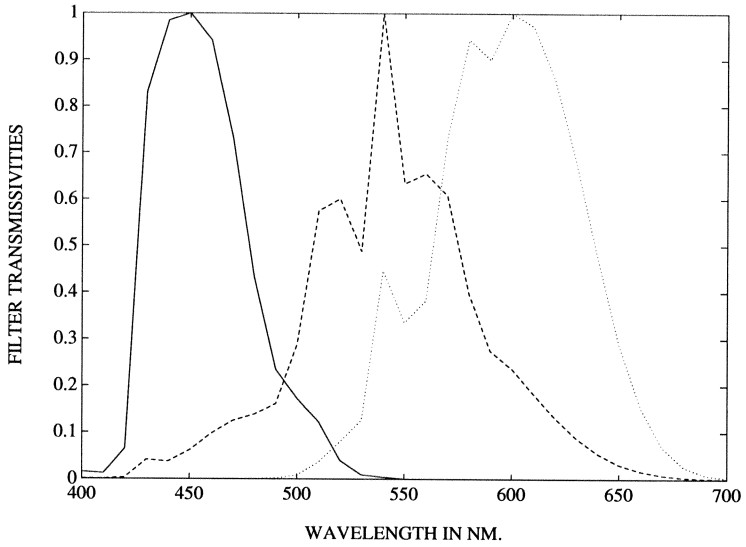

Figure 4.16: Designed Effective Scanning Filters for Sum-of-Gaussian Model and Illuminant 2

Other initial points provided slightly higher values of the measure. For example, starting with the initial estimate listed as Filter Set 1 in Table 4.4, the filter estimates of Table 4.4 were obtained. The estimates are plotted in Fig. 4.17 and Fig. 4.18. Note that the values of the measure are larger than the corresponding values of the measure listed in Table 4.3 for the sum-of-gaussian model for either illuminant, and that the values of E and E_{max} are considerably smaller for Illuminant 1. The fact that the ΔE_{Lab} errors are not perceptible implies that it is not worthwhile to increase the number of parameters further. Also, the sum of a larger number of gaussians could result in a multi-modal curve which might be difficult to fabricate.

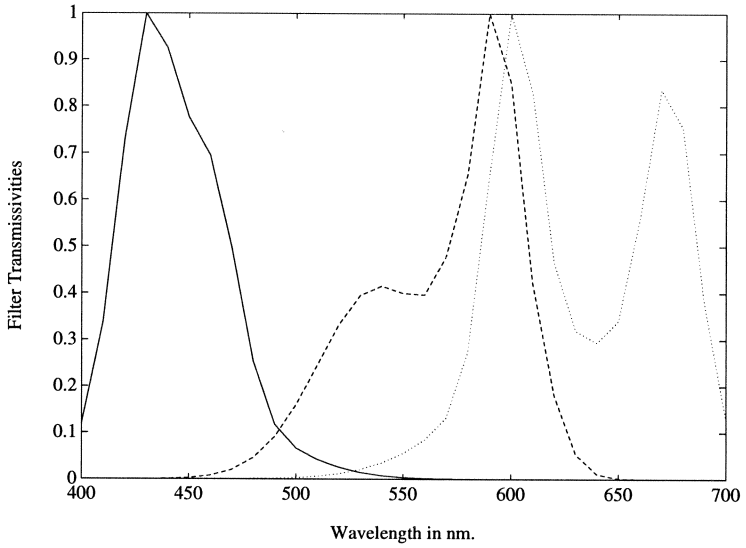

Figure 4.17: Designed Filters for Three-Gaussian Model and Illuminant 1

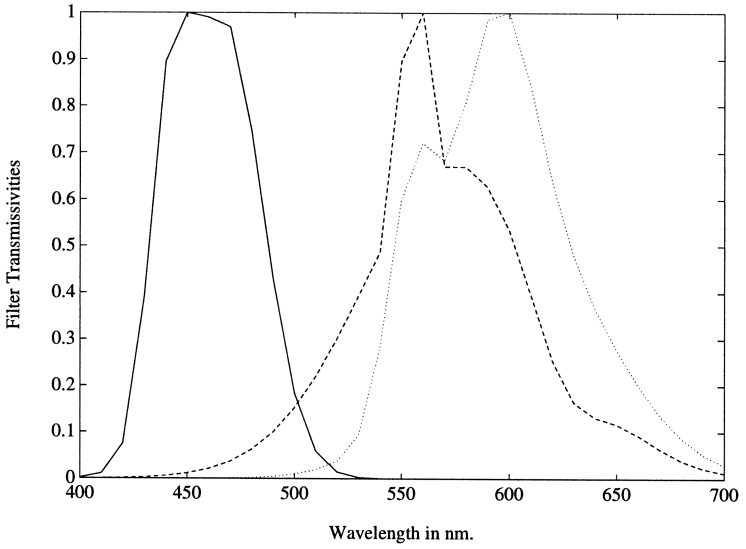

Figure 4.18: Designed Filters for Three-Gaussian Model and Illuminant 2

Table 4.4: Parameters for Sum-of-Three-Gaussian Filter model

Filter Set	Illuminant	ν	Filter No. 1	Filter No. 2	Filter No. 3	E	E_{max}
1	Initial Estimate		$\mu_{11} = 400.0$ $\sigma_{11} = 20.0$ $\mu_{12} = 420.0$ $\sigma_{12} = 20.0$ $\mu_{13} = 440.0$ $\sigma_{13} = 20.0$ $\alpha_{12} = 1.0$ $\alpha_{13} = 1.0$	$\mu_{21} = 500.0$ $\sigma_{21} = 20.0$ $\mu_{22} = 520.0$ $\sigma_{22} = 20.0$ $\mu_{23} = 540.0$ $\sigma_{23} = 20.0$ $\alpha_{22} = 1.0$ $\alpha_{23} = 1.0$	$\mu_{31} = 600.0$ $\sigma_{31} = 20.0$ $\mu_{32} = 620.0$ $\sigma_{32} = 20.0$ $\mu_{33} = 640.0$ $\sigma_{33} = 20.0$ $\alpha_{32} = 1.0$ $\alpha_{33} = 1.0$		
2	1	0.9951	$\mu_{11} = 430.4$ $\sigma_{11} = 13.2$ $\mu_{12} = 450.7$ $\sigma_{12} = 36.2$ $\mu_{13} = 460.2$ $\sigma_{13} = 12.6$ $\alpha_{12} = 0.1898$ $\alpha_{13} = 0.5656$	$\mu_{21} = 592.9$ $\sigma_{21} = 16.3$ $\mu_{22} = 538.3$ $\sigma_{22} = 27.8$ $\mu_{23} = 594.3$ $\sigma_{23} = 4.7$ $\alpha_{22} = 0.5832$ $\alpha_{23} = 0.4971$	$\mu_{31} = 626.7$ $\sigma_{31} = 41.9$ $\mu_{32} = 601.3$ $\sigma_{32} = 10.9$ $\mu_{33} = 674.1$ $\sigma_{33} = 11.8$ $\alpha_{32} = 0.2570$ $\alpha_{33} = 0.2371$	0.23	1.19
3	2	0.9722	$\mu_{11} = -144.1$ $\sigma_{11} = 33.0$ $\mu_{12} = 441.1$ $\sigma_{12} = 8.9$ $\mu_{13} = 466.2$ $\sigma_{13} = 18.4$ $\alpha_{12} = 0.8158$ $\alpha_{13} = 1.4860$	$\mu_{21} = 575.5$ $\sigma_{21} = 43.8$ $\mu_{22} = 624.8$ $\sigma_{22} = 15.6$ $\mu_{23} = 555.1$ $\sigma_{23} = 3.6$ $\alpha_{22} = -0.2314$ $\alpha_{23} = 1.3712$	$\mu_{31} = 593.6$ $\sigma_{31} = 17.1$ $\mu_{32} = 554.8$ $\sigma_{32} = 10.6$ $\mu_{33} = 608.3$ $\sigma_{33} = 38.5$ $\alpha_{32} = 0.8429$ $\alpha_{33} = 0.8846$	0.73	3.0

4.4.5 Single-Raised-Cosine Model

The parameters obtained for the single-raised-cosine model of equation (4.7) for Illuminants 1 and 2 are tabulated in Table 4.5. Also tabulated are the maximum ΔE_{Lab} error, E_{max}, the average ΔE_{Lab} error, E, and the measure of the optimal sets of filters. The designed filters are plotted in Figs. 4.19 and 4.20 respectively.

Table 4.5: Parameters for the Single Raised-Cosine Filter Model

Filter Set	Illuminant	ν	Filter No. 1	Filter No. 2	Filter No. 3	E	E_{max}
1	1	0.9415	$\zeta_1 = 437.3$ $T_1 = 137.4$	$\zeta_2 = 548.5$ $T_2 = 181.1$	$\zeta_3 = 608.4$ $T_3 = 105.7$	1.68	8.12
2	2	0.9445	$\zeta_1 = 460.2$ $T_1 = 109.5$	$\zeta_2 = 551.9$ $T_2 = 185.9$	$\zeta_3 = 598.9$ $T_3 = 160.3$	0.89	2.40

4.4.6 Sum-of-Raised-Cosine Model

The parameters obtained for the sum of raised-cosines model of equation (4.8) are tabulated in Table 4.6, along with average and maximum ΔE_{Lab} errors E and E_{max} respectively. The filters are shown in Figs. 4.21 and 4.22 respectively.

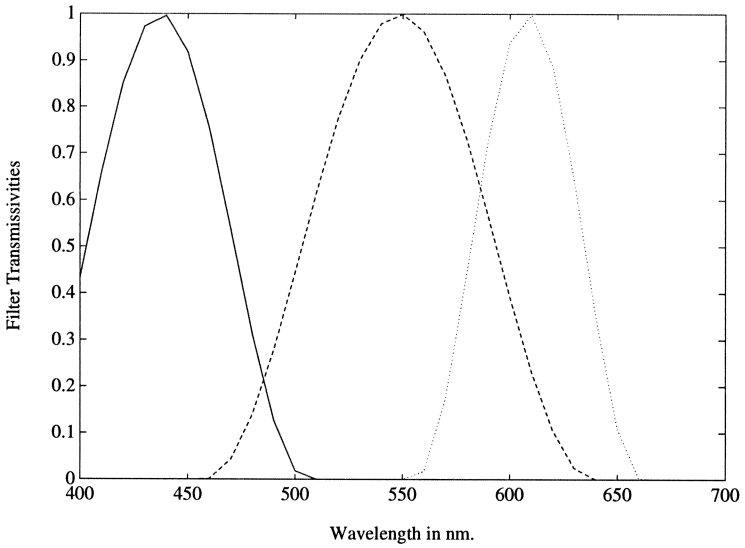

Figure 4.19: Designed Filters for Single-Raised-Cosine Model and Illuminant 1

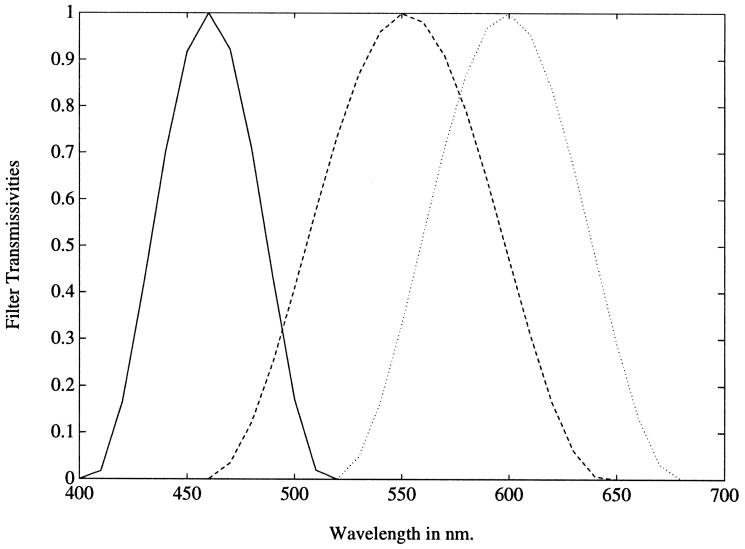

Figure 4.20: Designed Filters for Single-Raised-Cosine Model and Illuminant 2

Table 4.6: Parameters for the Sum-of-Raised-Cosines Filter Model

Illuminant	ν	Filter No. 1	Filter No. 2	Filter No. 3	E	E_{max}
1	0.9887	$T_{11} = 127.4$ $\zeta_{11} = 442.4$ $T_{12} = 30.7$ $\zeta_{12} = 430.6$ $\alpha_1 = 0.3380$	$T_{21} = 63.1$ $\zeta_{21} = 594.0$ $T_{22} = 17.0$ $\zeta_{22} = 547.2$ $\alpha_2 = 0.6441$	$T_{31} = 56.7$ $\zeta_{31} = 601.2$ $T_{32} = 287.8$ $\zeta_{32} = 659.1$ $\alpha_3 = 0.4933$	0.53	1.69
2	0.9607	$T_{11} = 98.7$ $\zeta_{11} = 461.8$ $T_{12} = 54.5$ $\zeta_{12} = 465.1$ $\alpha_1 = -0.3478$	$T_{21} = 118.9$ $\zeta_{21} = 560.4$ $T_{22} = 92.3$ $\zeta_{22} = 501.7$ $\alpha_2 = 0.4349$	$T_{31} = 135.9$ $\zeta_{31} = 614.8$ $T_{32} = 121.4$ $\zeta_{32} = 577.1$ $\alpha_3 = 0.9501$	0.48	1.46

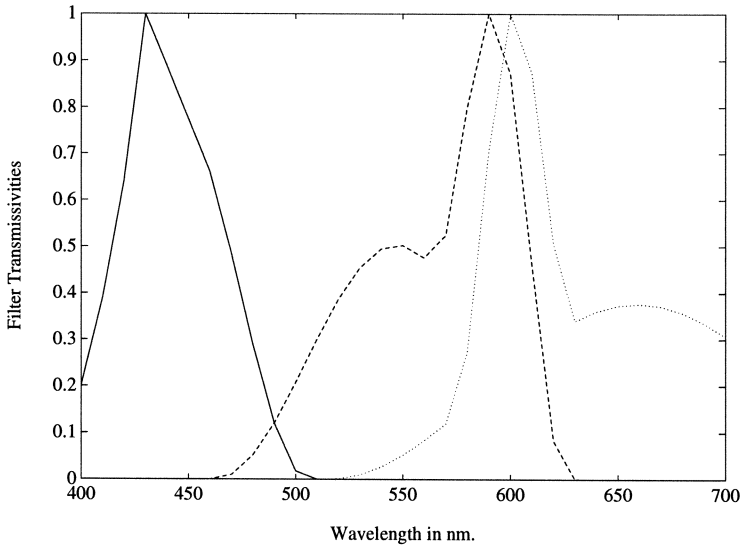

Figure 4.21: Designed Filters for Sum-of-Raised-Cosine Model and Illuminant 1

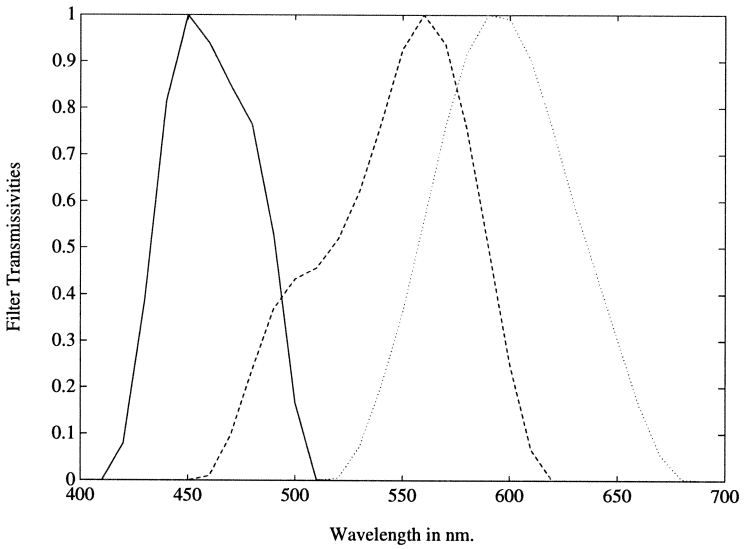

Figure 4.22: Designed Filters for Sum-of-Raised-Cosine Model and Illuminant 2

4.4.7 Exponential-Cosine Model

The parameters obtained for the exponential-cosine model of equation (4.9) for Illuminants 1 and 2 are tabulated in Table 4.7. Also tabulated are the maximum ΔE_{Lab} error, E_{max}, the average ΔE_{Lab} error, E, and the measure of the optimal sets of filters. The designed filters are plotted in Figs. 4.23 and 4.24 respectively.

Table 4.7: Parameters for the Exponential Cosine Filter Model

Illuminant	ν	Filter 1	Filter 2	Filter 3	E	E_{max}
1	0.9544	$\zeta_1 = 437.8$ $T_1 = 255.3$ $a_1 = 2.5936$	$\zeta_2 = 541.9$ $T_2 = 176.1$ $a_2 = 0.7777$	$\zeta_3 = 606.4$ $T_3 = 141.2$ $a_3 = 1.9117$	1.95	10.47
2	0.9303	$\zeta_1 = 459.4$ $T_1 = 221.3$ $a_1 = 2.2221$	$\zeta_2 = 566.9$ $T_2 = 233.7$ $a_2 = 1.0725$	$\zeta_3 = 603.8$ $T_3 = 167.7$ $a_3 = 1.0357$	1.71	7.24

4.4.8 Discussion of Results

The single-gaussian and the raised-cosine models give similar results. The maximum ΔE_{Lab} error for the best single-raised-cosine model is slightly lower than the corresponding error for the single-gaussian model for Illuminant 1. The exponential-cosine filters are worse in performance than both single-gaussian and single-raised-cosine as indicated by both average and maximum ΔE_{Lab} errors, in spite of the fact that the exponential-cosine model involves more parameters (nine) than the other two models, which involve six parameters. It may be noted that the slightly higher value for the measure obtained for the exponential-cosine model and Illuminant 1 is not indicative of the higher values of the ΔE_{Lab} errors as compared to the single-raised-cosine model

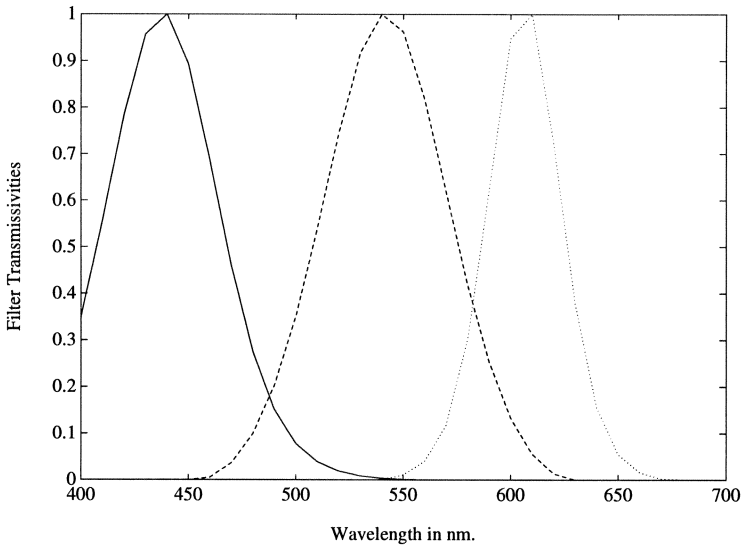

Figure 4.23: Designed Filters for Exponential-Cosine Model and Illuminant 1

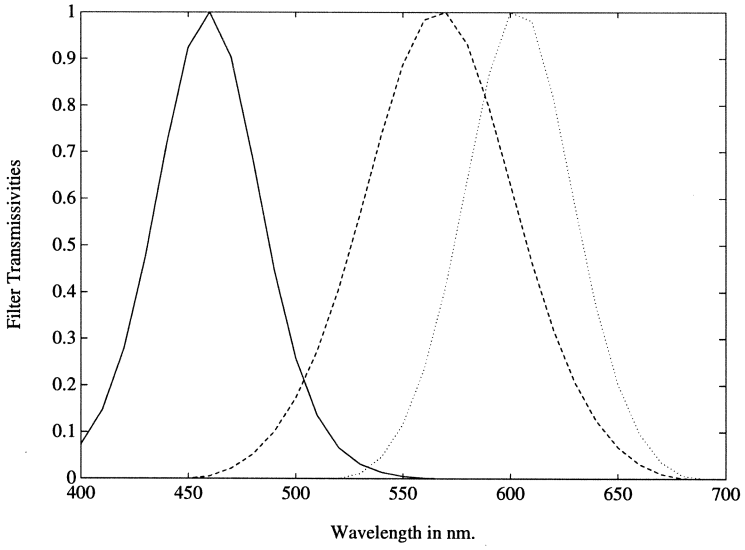

Figure 4.24: Designed Filters for Exponential-Cosine Model and Illuminant 2

for the same illuminant. The single-gaussian model provides the highest values of the measure for both illuminants.

The sum-of-raised-cosines model and the sum-of-gaussians model both provide similar results. The sum-of-raised-cosines model provides an imperceptible maximum ΔE_{Lab} error for Illuminant 2 which is not true of the sum-of-gaussians model. The maximum ΔE_{Lab} errors for the sum-of-gaussians model and the sum-of-raised-cosines model are far smaller than the corresponding errors for the single-gaussian, single-raised-cosine and exponential-cosine models (except the unusually high value of the maximum ΔE_{Lab} error for Illuminant 2 and the sum-of-gaussian model), justifying the increase in parameters from six and nine to fifteen.

The optimizations reported were performed with several initial points. The results obtained with the different initial points varied somewhat in the parameters, and the resulting optimal measure values were either clearly not global optima or within 5% of one another. It is suggested that the optimization program should be run with a number of initial points to allow for a higher probability of obtaining optimal results. There are instances when a higher measure does not imply a lower ΔE_{Lab} error. This is not particularly surprising, and the small differences imply that it is not critical for a coarse optimization. The next section presents a method by which filter sets with optimal ΔE_{Lab} values may be obtained.

4.5 The Jacobian and its Use in Trimming Optimal Results

The experimental results of section 4.4 indicate that filters with fairly high values of the measure do produce reproductions with perceptible errors, as indicated by the average and maximum ΔE_{Lab} error over the Munsell chip set. As mentioned in section

3.5.4, it is impractical to use the average square ΔE_{Lab} error over a data set as an optimization criterion. Once a set of 'optimal' (with respect to the data-independent measure of Chapter 3) filters are found, it may be feasible to 'trim' these filters using the average square ΔE_{Lab} error as an optimization criterion. Such trimming is clearly dependent on the data set.

Once smooth filters with fairly high values of the optimization criterion are obtained, the method of steepest descent [19, pg. 285], may be used to trim the filters and obtain smooth filters with lower average square ΔE_{Lab} error over a particular data set. The resulting filters will not be parametrizable, in general. The method of steepest descent with initial points consisting of smooth filter sets of fairly high measure is an efficient way of imposing the smoothness criterion. This section deals with the trimming of some of the filters designed in section 4.4 to produce smooth filters with lower average square ΔE_{Lab} errors over a particular data set. Filters are also trimmed for one filter model to produce a filter set of optimum measure, ν. This experiment is performed to demonstrate how the measure can change due to trimming with respect to the measure, and to compare such a change with a change in ΔE_{Lab} error due to trimming with respect to this error.

The matrices $\mathbf{M}_H$, $\mathbf{R}$ and $\mathbf{V}$ will be assumed full rank. This simply means that the effective scanning filters are linearly independent, that the columns of $\mathbf{V}$ are linearly independent and that $\mathbf{R}$ is invertible. The assumption implies that $\mathbf{M}_H^T\mathbf{R}\mathbf{M}_H$, $\mathbf{M}_H^T\mathbf{M}_H$ and $\mathbf{V}^T\mathbf{V}$ are invertible.

4.5.1 Notation

The notation followed is that of Magnus and Neudecker [21]. Given a scalar function f of an $m \times n$ matrix $\mathbf{X}$, the following $m \times n$ matrix will denote the operation of

term-by-term differentiation:

$$\frac{\partial f}{\partial \mathbf{X}} = [\frac{\partial f}{\partial \mathbf{X}_{ij}}]$$

Thus the ij^{th} element of $\frac{\partial f}{\partial \mathbf{X}}$ is the partial derivative of the function f with respect to the ij^{th} element of $\mathbf{X}$. In the specific case of a scalar function $f(\mathbf{x})$ of a column vector $\mathbf{x}$, the following column vector will denote term-by-term differentiation:

$$\frac{\partial f}{\partial \mathbf{x}} = [\frac{\partial f}{\partial \mathbf{x}_i}]$$

If $\mathbf{x} = [\mathbf{x}_1, \mathbf{x}_2, ..., \mathbf{x}_q]$ is a row vector, the row vector

$$\frac{\partial f}{\partial \mathbf{x}} = [\frac{\partial f}{\partial \mathbf{x}_1}, \frac{\partial f}{\partial \mathbf{x}_2}, ..., \frac{\partial f}{\partial \mathbf{x}_q}]$$

denotes term-by-term differentiation. Given a matrix with q columns,

$$\mathbf{X} = [\mathbf{x}_1, \mathbf{x}_2, ...\mathbf{x}_q]$$

the vector of stacked columns,

$$vec(\mathbf{X}) = \begin{bmatrix} \mathbf{x}_1 \\ \mathbf{x}_2 \\ \vdots \\ \mathbf{x}_q \end{bmatrix}$$

defines a vector representation of $\mathbf{X}$. The Jacobian of a scalar function f of the vector $vec\ \mathbf{X}$ is defined as

$$\mathbf{D}f(vec\ \mathbf{X}) = \frac{\partial f}{\partial (vec\mathbf{X})^T} = (vec[\frac{\partial f}{\partial \mathbf{X}_{ij}}])^T \tag{4.10}$$

Notice that the Jacobian in this case is a row vector, and that it is the transpose of the gradient vector. If df represents the differential of f and $d\mathbf{X} = [d\mathbf{X}_{ij}]$ the

differential of $\mathbf{X}$, then [21]

$$df = Trace\mathbf{J}^T d\mathbf{X} \Leftrightarrow vec\mathbf{J} = (\mathbf{D}f(\mathbf{X}))^T \tag{4.11}$$

and

$$df = \mathbf{D}f(\mathbf{X}) vec\, d\mathbf{X} \tag{4.12}$$

In the specific case of a scalar function f of a column vector $\mathbf{x}$, the row vector

$$\mathbf{D}f(\mathbf{x}) = \frac{\partial f}{\partial \mathbf{x}^T} = \left[\frac{\partial f}{\partial \mathbf{x}_i}\right]^T$$

is defined as the Jacobian of f with respect to $\mathbf{x}$. If $d\mathbf{x} = [d\mathbf{x}_i]$ represents the differential of $\mathbf{x}$, then [21]

$$df = (\mathbf{A}(\mathbf{x}))^T d\mathbf{x} <=> \mathbf{A}(\mathbf{x}) = (\mathbf{D}f(\mathbf{x}))^T \tag{4.13}$$

With the above notation, one variation of the method of steepest descent for a scalar function of a matrix $\mathbf{X}$ is [19, pg. 285]

$$vec\mathbf{X}_{k+1} = vec\mathbf{X}_k - \alpha_k \mathbf{D}(f)^T(\mathbf{X}_k) \tag{4.14}$$

In the particular application of finding $\mathbf{M}$ such that the average ΔE_{Lab} error over a data set (or data-independent measure ν) is optimum, the average ΔE_{Lab} error (or data-independent measure ν) is the scalar function of matrix $\mathbf{M}$.

The following laws of matrix differentials are used in the next sections to obtain the required differentials:

$$d(a\mathbf{X}) = ad\mathbf{X} \tag{4.15}$$

$$d(\mathbf{AX}) = \mathbf{A}d\mathbf{X}$$

$$d(\mathbf{XY}) = \mathbf{X}d\mathbf{Y} + d\mathbf{X}\mathbf{Y}$$

$$d(trace\mathbf{X}) = trace\ d\mathbf{X}$$

$$d(\mathbf{X}^{-1}) = -\mathbf{X}^{-1}(d\mathbf{X})\mathbf{X}^{-1}$$

$$d(\mathbf{X}^T) = (d\mathbf{X})^T$$

4.5.2 Calculation of the Jacobian for the Data-Independent Measure

It can be shown that (see Appendix, Theorem 8)

$$d(\nu(\mathbf{A}_L, \mathbf{M}_H)) = \frac{Trace2(\mathbf{M}_H^T\mathbf{M}_H)^{-1}\mathbf{M}_H^T P_V(\mathbf{I} - P_{M_H})\mathbf{H}d\mathbf{M}}{3} \tag{4.16}$$

where d represents the differential. From equation (4.11), [21]

$$\mathbf{D}(\nu)(\mathbf{M}) = \{vec(\frac{2\mathbf{H}(\mathbf{I} - P_{M_H})P_V\mathbf{M}_H(\mathbf{M}_H^T\mathbf{M}_H)^{-1}}{3})\}^T \tag{4.17}$$

4.5.3 Calculation of the Jacobian for the Average ΔE_{Lab} Error Over a Given Data Set

Let $\hat{\mathbf{t}}(\mathbf{f}) = [x,\ y,\ z]^T$ be the estimated CIE tristimulus values for the reflectance signal $\mathbf{f}$. Let $\mathcal{F}(\hat{\mathbf{t}}(\mathbf{f})) = [L,\ a,\ b]^T$ be the transformed (estimated) tristimulus vector in CIELab space. Let $\mathbf{t}(\mathbf{f}) = [x_f,\ y_f,\ z_f]^T$ be the actual CIE tristimulus values for the reflectance signal $\mathbf{f}$ and $\mathcal{F}(\mathbf{t}(\mathbf{f})) = [L_f,\ a_f,\ b_f]^T$ be the transformed (actual) tristimulus vector in CIELab space. Let $\Delta E_{Lab}(\mathbf{f})$ be the ΔE_{Lab} error for reflectance spectrum $\mathbf{f}$. Then, the average square ΔE_{Lab} error over a data set with n points is:

$$\frac{\sum_{\mathbf{f}} \Delta E_{Lab}^2(\mathbf{f})}{n} = \frac{\sum_{\mathbf{f}}[(L - L_f)^2 + (a - a_f)^2 + (b - b_f)^2]}{n}$$

where $\sum_{\mathbf{f}}$ represents the sum over the data set. Further, the first differential of the average square ΔE_{Lab} error over a data set with n points is:

$$d(\frac{\sum_{\mathbf{f}} \Delta E^2_{Lab}(\mathbf{f})}{n}) \;=\; \frac{\sum_{\mathbf{f}} 2[(L \;-\; L_f)dL \;+\; (a \;-\; a_f)da \;+\; (b \;-\; b_f)db]}{n}$$

or

$$d(\frac{\sum_{\mathbf{f}} \Delta E^2_{Lab}(\mathbf{f})}{n}) \;=\; \frac{\sum_{\mathbf{f}} Trace2[(L \;-\; L_f),\; (a \;-\; a_f),\; (b \;-\; b_f)]d\mathcal{F}(\hat{\mathbf{t}}(\mathbf{f}))}{n}$$

Let

$$\mathbf{c}(\mathbf{f}) \;=\; 2[(L \;-\; L_f),\; (a \;-\; a_f),\; (b \;-\; b_f)]^T \tag{4.18}$$

Then,

$$d(\frac{\sum_{\mathbf{f}} \Delta E^2_{Lab}(\mathbf{f})}{n}) \;=\; \frac{Trace \sum_{\mathbf{f}} \mathbf{c}^T(\mathbf{f})d\mathcal{F}(\hat{\mathbf{t}}(\mathbf{f}))}{n} \tag{4.19}$$

If $[x_n,\; y_n,\; z_n]^T$ represents the white point, recall that (from section 1.1.2, equation (1.4))

$$L \;=\; 116(\frac{y}{y_n})^{1/3} \;-\; 16$$

$$a \;=\; 500((\frac{x}{x_n})^{1/3} \;-\; (\frac{y}{y_n})^{1/3})$$

and

$$b \;=\; 200((\frac{y}{y_n})^{1/3} \;-\; (\frac{z}{z_n})^{1/3})$$

This implies that

$$dL \;=\; \frac{116\; dy}{3(y^2 y_n)^{1/3}}$$

$$da \;=\; \frac{500\; dx}{3(x^2 x_n)^{1/3}} \;-\; \frac{500\; dy}{3(y^2 y_n)^{1/3}}$$

and

$$db = \frac{200\ dy}{3(y^2 y_n)^{1/3}} - \frac{200\ dz}{3(z^2 z_n)^{1/3}}$$

which may be written in matrix notation as

$$d\mathcal{F}(\hat{\mathbf{t}}(\mathbf{f})) = \begin{bmatrix} 0 & \frac{116}{3(y^2 y_n)^{1/3}} & 0 \\ \frac{500}{3(x^2 x_n)^{1/3}} & \frac{-500}{3(y^2 y_n)^{1/3}} & 0 \\ 0 & \frac{200}{3(y^2 y_n)^{1/3}} & \frac{-200}{3(z^2 z_n)^{1/3}} \end{bmatrix} d\hat{\mathbf{t}}(\mathbf{f})$$

If

$$\boldsymbol{\Omega}(\mathbf{f}) = \begin{bmatrix} \frac{1}{3(x^2 x_n)^{1/3}} & 0 & 0 \\ 0 & \frac{1}{3(y^2 y_n)^{1/3}} & 0 \\ 0 & 0 & \frac{1}{3(z^2 z_n)^{1/3}} \end{bmatrix} \tag{4.20}$$

then,

$$d\mathcal{F}(\hat{\mathbf{t}}(\mathbf{f})) = \boldsymbol{\Upsilon}\boldsymbol{\Omega}(\mathbf{f}) d\hat{\mathbf{t}}(\mathbf{f}) \tag{4.21}$$

where the matrix Υ is defined in section 1.1.2, equation (1.5). Differentiating the expression for the corrected tristimulus estimate of equation (3.8) using the laws of matrix differentiation in equations (4.15), gives

$$\begin{aligned} d\hat{\mathbf{t}}(\mathbf{f}) = {} & \mathbf{A}^T\mathbf{R}d\mathbf{M}_H(\mathbf{M}_H^T\mathbf{R}\mathbf{M}_H)^{-1}\mathbf{M}_H^T\mathbf{f} - \\ & \mathbf{A}^T\mathbf{R}\mathbf{M}_H(\mathbf{M}_H^T\mathbf{R}\mathbf{M}_H)^{-1}\mathbf{M}_H^T\mathbf{R}d\mathbf{M}_H(\mathbf{M}_H^T\mathbf{R}\mathbf{M}_H)^{-1}\mathbf{M}_H^T\mathbf{f} - \\ & \mathbf{A}^T\mathbf{R}\mathbf{M}_H(\mathbf{M}_H^T\mathbf{R}\mathbf{M}_H)^{-1}d\mathbf{M}_H^T\mathbf{R}\mathbf{M}_H(\mathbf{M}_H^T\mathbf{R}\mathbf{M}_H)^{-1}\mathbf{M}_H^T\mathbf{f} + \\ & \mathbf{A}^T\mathbf{R}\mathbf{M}_H(\mathbf{M}_H^T\mathbf{R}\mathbf{M}_H)^{-1}d\mathbf{M}_H^T\mathbf{f} \end{aligned} \tag{4.22}$$

Using equations (4.22), (4.21) and (4.19), and using $Trace\mathbf{XYZ} = Trace\mathbf{ZXY}$ to obtain an expression of the form $Trace\mathbf{C}d\mathbf{M}_H + d\mathbf{M}_H^T\mathbf{G}$ gives

$d(\frac{\sum_{\mathbf{f}} \Delta E_{Lab}^2(\mathbf{f})}{n}) =$

$$\frac{1}{n} Trace(\mathbf{M}_H^T\mathbf{R}\mathbf{M}_H)^{-1}\mathbf{M}_H^T\mathbf{f}\mathbf{c}^T\boldsymbol{\Upsilon}\boldsymbol{\Omega}\mathbf{A}^T\mathbf{R}(\mathbf{I} - \mathbf{M}_H(\mathbf{M}_H^T\mathbf{R}\mathbf{M}_H)^{-1}\mathbf{M}_H^T\mathbf{R})d\mathbf{M}_H$$

$$+ d\mathbf{M}_H^T(\mathbf{I} - \mathbf{R}\mathbf{M}_H(\mathbf{M}_H^T\mathbf{R}\mathbf{M}_H)^{-1}\mathbf{M}_H^T)\mathbf{f}\mathbf{c}^T\boldsymbol{\Upsilon}\boldsymbol{\Omega}\mathbf{A}^T\mathbf{R}\mathbf{M}_H(\mathbf{M}_H^T\mathbf{R}\mathbf{M}_H)^{-1}$$

Using $Trace\mathbf{X}^T = Trace\mathbf{X}$ produces the result:

$d(\frac{\sum_{\mathbf{f}} \Delta E_{Lab}^2(\mathbf{f})}{n}) =$

$$Trace(\mathbf{M}_H^T\mathbf{R}\mathbf{M}_H)^{-1}\mathbf{M}_H^T(\frac{\sum_{\mathbf{f}} \boldsymbol{\Xi}(\mathbf{f})}{n})(\mathbf{I} - \mathbf{M}_H(\mathbf{M}_H^T\mathbf{R}\mathbf{M}_H)^{-1}\mathbf{M}_H^T\mathbf{R})d\mathbf{M}_H \quad (4.23)$$

where

$$\boldsymbol{\Xi}(\mathbf{f}) = \mathbf{f}\mathbf{c}^T(\mathbf{f})\boldsymbol{\Upsilon}\boldsymbol{\Omega}(\mathbf{f})\mathbf{A}^T\mathbf{R} + \mathbf{R}\mathbf{A}\boldsymbol{\Omega}(\mathbf{f})\boldsymbol{\Upsilon}^T\mathbf{c}(\mathbf{f})\mathbf{f}^T \quad (4.24)$$

From equations (4.11) and (4.23) and using the fact that $d\mathbf{M}_H = \mathbf{H}d\mathbf{M}$,

$$\mathbf{D}\frac{\sum_{\mathbf{f}} \Delta E_{Lab}^2(\mathbf{f})}{n}$$

$$= \{vec\mathbf{H}(\mathbf{I} - \mathbf{R}\mathbf{M}_H(\mathbf{M}_H^T\mathbf{R}\mathbf{M}_H)^{-1}\mathbf{M}_H^T)(\frac{\sum_{\mathbf{f}} \boldsymbol{\Xi}(\mathbf{f})}{n})\mathbf{M}_H(\mathbf{M}_H^T\mathbf{R}\mathbf{M}_H)^{-1}\}^T$$

is the Jacobian of the average square ΔE_{Lab} error over a given data set. The relevant equation for the method of steepest descent is, from equation (4.14),

$$vec\mathbf{M}_{k+1} = vec\mathbf{M}_k - \alpha_k\mathbf{D}^T\frac{\sum_{\mathbf{f}} \Delta E_{Lab}^2(\mathbf{f})}{n}(\mathbf{M}_k)$$

4.5.4 Experimental Results

The results of trimming the designed filters with respect to both the data-independent measure and the mean square ΔE_{Lab} error are presented in this section.

Trimming with Respect to the Data-Independent Measure ν

Examples of trimming with respect to the data-independent measure ν are presented in Fig 4.25 and in Fig. 4.26. The former represents the filters of Figs. 4.9-4.11

trimmed with respect to the data-independent measure and is referred to as Set 1. The latter represents the filters of Figs. 4.12-4.14 trimmed with respect to the data-independent measure and is referred to as Set 2. A comparison of the errors before and after trimming are presented in Table 4.8. In Table 4.8, the measure $\nu(\mathbf{A}, \mathbf{M}_H)$ is denoted ν, the average ΔE_{Lab} error E, the maximum ΔE_{Lab} error E_{max}, and the root mean square ΔE_{Lab} error RMS. The root mean square ΔE_{Lab} error is presented here to allow comparison with the trimming with respect to mean square ΔE_{Lab} error, results of which are presented later.

Table 4.8: Comparison Between Errors Before and After Filter-Trimming With Respect to Measure ν

Filter Model	Before Trimming				After Trimming			
	ν	E	E_{max}	RMS	ν	E	E_{max}	RMS
Sum-of-Gaussian(Set 1)	0.9928	0.46	1.71	0.60	0.9994	0.28	1.23	0.38
Sum-of-Gaussian(Set 2)	0.9832	1.25	7.46	1.89	0.9988	0.51	3.38	0.79

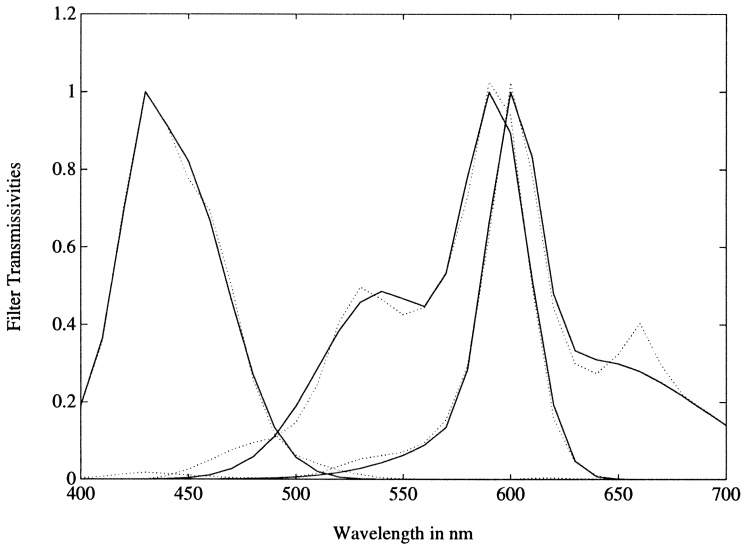

Figure 4.25: Trimmed Filters (Data-Independent Measure) for Sum-of-Gaussian Model and Illuminant 1

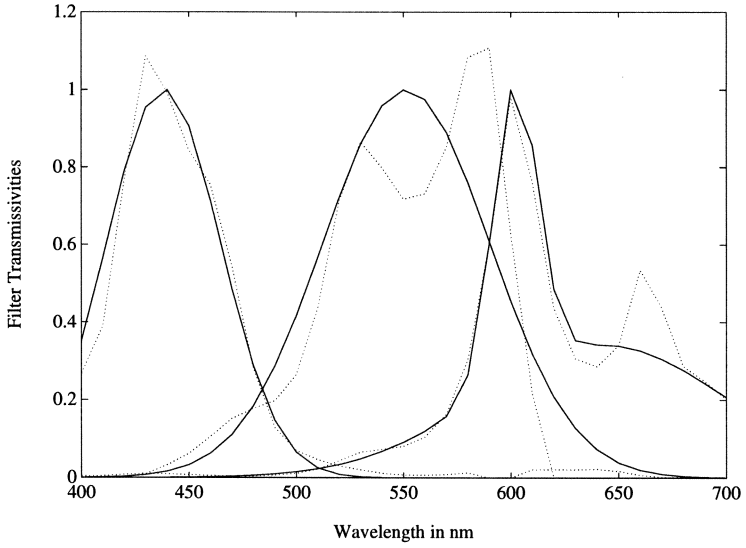

Figure 4.26: Trimmed Filters (Data-Independent Measure) for Sum-of-Gaussian Model and Illuminant 1

Trimming with Respect to Mean Square ΔE_{Lab} Error

The Jacobian of the average square ΔE_{Lab} error over the Munsell chip set was used to trim the designed filters shown in Figs. 4.5; 4.6-4.8; 4.9-4.11; and 4.23. The results of trimming the single-gaussian design of Fig. 4.5 are shown in Figs. 4.27-4.29. The results of trimming the single-gaussian design of Figs 4.6-4.8 are shown in Fig. 4.30. The results of trimming the sum-of-gaussian filters of Figs. 4.9-4.11 are shown in Fig. 4.31. The results of trimming the exponential-cosine filters of Fig 4.23 are shown in Figs. 4.32-4.34.

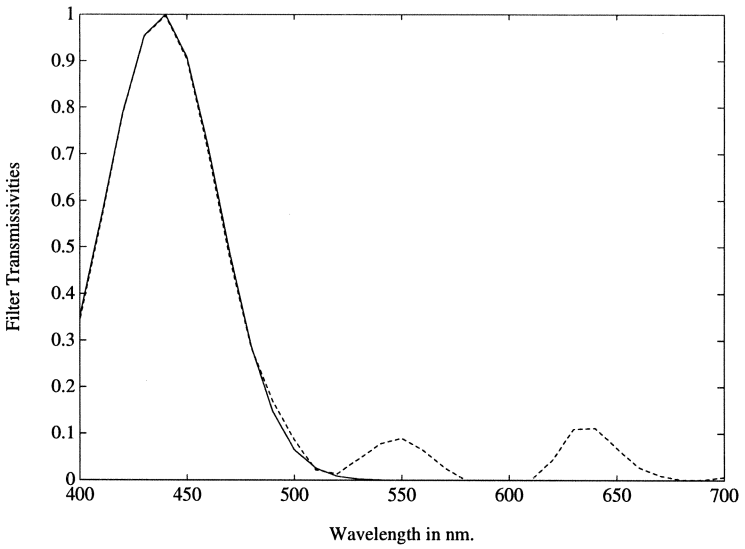

Figure 4.27: Trimmed Blue Filter (Mean Square ΔE_{Lab} Error) for Single-Gaussian Model and Illuminant 1

Table 4.9 lists the different error measures before and after trimming. It is clear that trimming improves the general characteristics of the filter set. The single-gaussian filter sets and the exponential-cosine set have shown more improvement

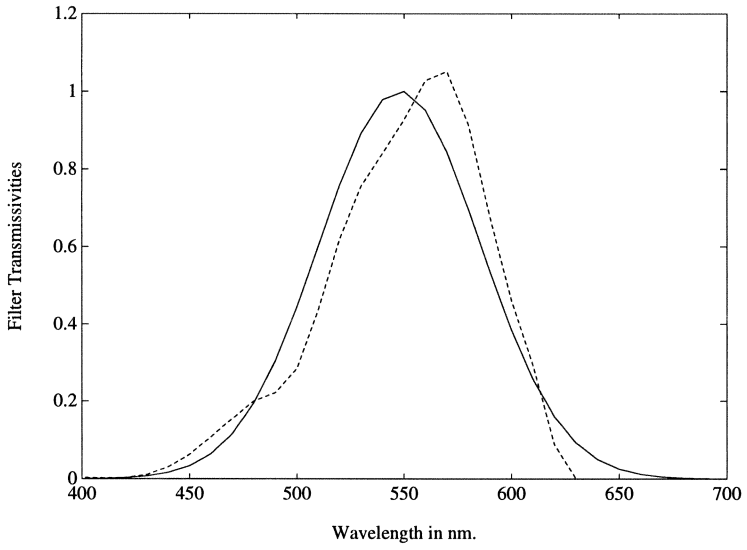

Figure 4.28: Trimmed Green Filter (Mean Square ΔE_{Lab} Error) for Single-Gaussian Model and Illuminant 1

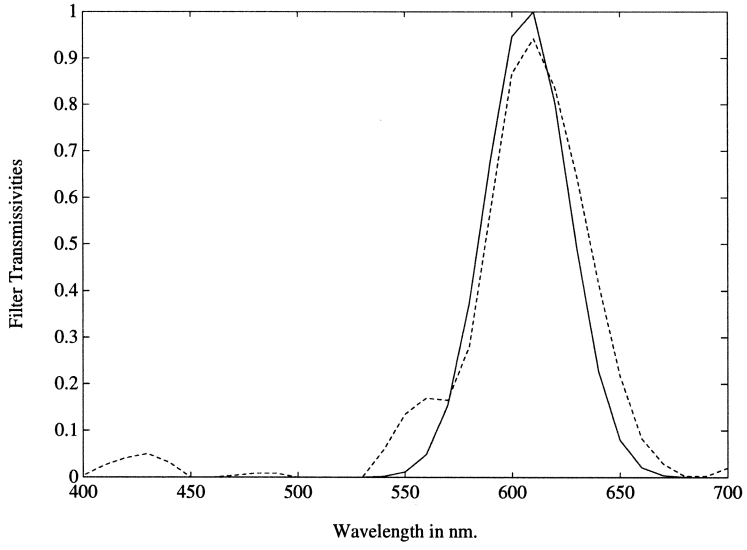

Figure 4.29: Trimmed Red Filter (Mean Square ΔE_{Lab} Error) for Single-Gaussian Model and Illuminant 1

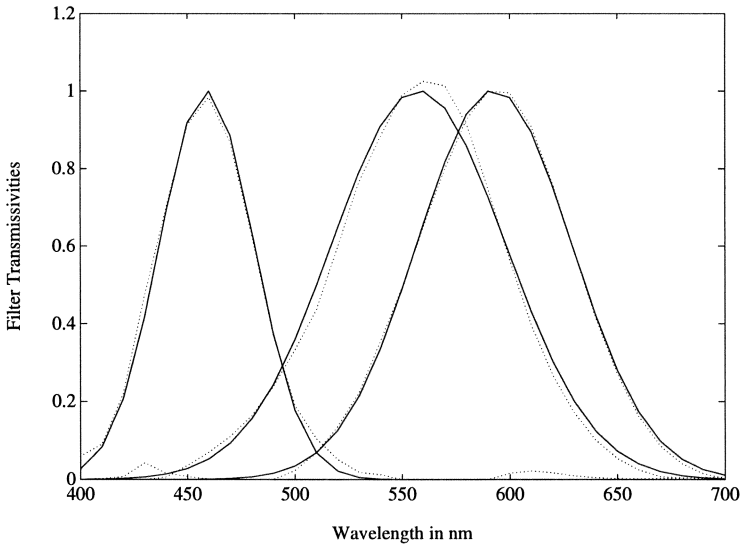

Figure 4.30: Trimmed Filters (Mean Square ΔE_{Lab} Error) for Single-Gaussian Model and Illuminant 2

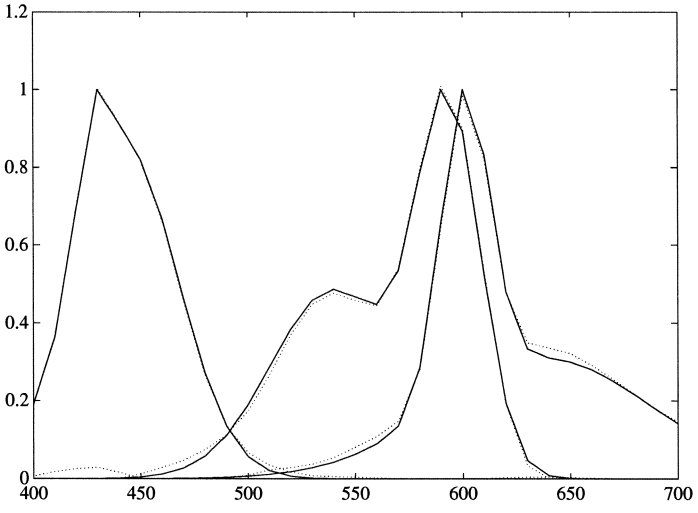

Figure 4.31: Trimmed Filters (Mean Square ΔE_{Lab} Error) for Sum-of-Gaussian Model and Illuminant 1

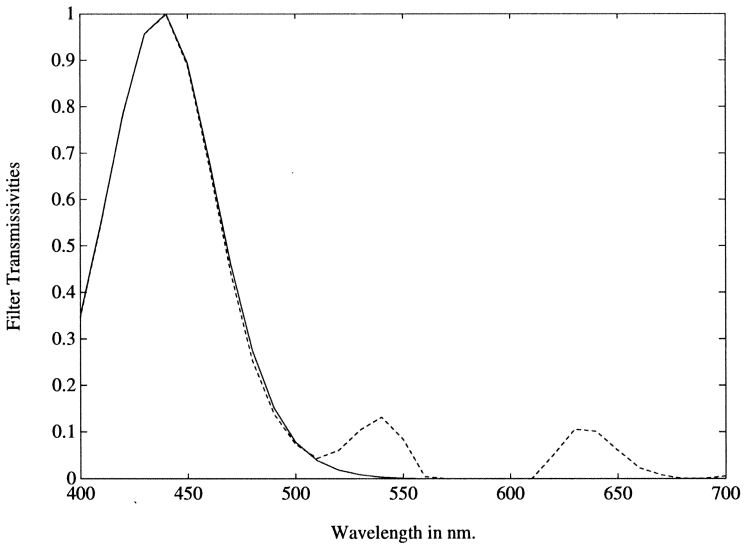

Figure 4.32: Trimmed Blue Filter (Mean Square ΔE_{Lab} Error) for Exponential Cosine Model and Illuminant 1

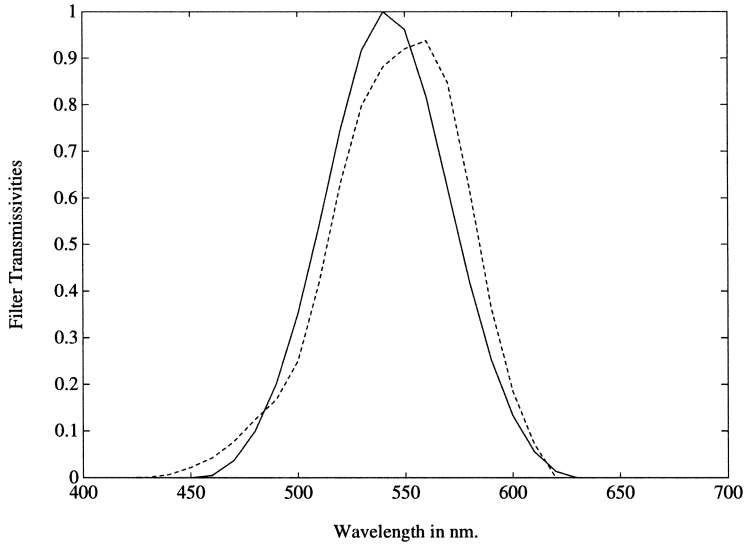

Figure 4.33: Trimmed Green Filter (Mean Square ΔE_{Lab} Error) for Exponential Cosine Model and Illuminant 1

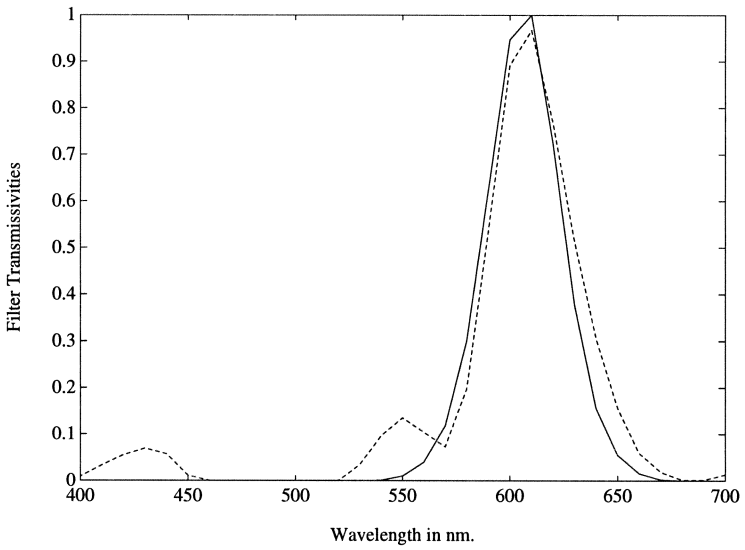

Figure 4.34: Trimmed Red Filter (Mean Square ΔE_{Lab} Error) for Exponential Cosine Model and Illuminant 1

than the sum-of-gaussian set. This is because the sum-of-gaussian set was a better set initially. In Table 4.9, the measure $\nu(\mathbf{A}, \mathbf{M}_H)$ is denoted ν, the average ΔE_{Lab} error E, the maximum ΔE_{Lab} error E_{max}, and the root mean square ΔE_{Lab} error RMS. The root mean square error is used here because it is the mean square error that is the optimization criterion for the trimming. The root mean square error should decrease on trimming, and the amount it decreases by indicates the effect of trimming on the original designs.

Note that the measure might decrease a little due to trimming, though the ΔE_{Lab} error is expected to decrease. This is because the measure is data-independent and is used to give an approximately optimum solution for the particular data set. Trimming is highly data-dependent and provides a closer-to-optimal solution for the particular data set. Notice that the ΔE_{Lab} error measures for the Sum-of-Gaussian model in

Table 4.9: Comparison Between Errors Before and After Filter-Trimming With Respect to Mean Square ΔE_{Lab} Error

Filter Model	Before Trimming				After Trimming			
	ν	E	E_{max}	RMS	ν	E	E_{max}	RMS
Single-Gaussian (Illuminant 1)	0.9556	1.75	9.16	2.49	0.9417	0.41	2.18	0.58
Single-Gaussian (Illuminant 2)	0.9485	0.84	2.46	1.09	0.9508	0.27	0.67	0.32
Sum-of-Gaussian	0.9928	0.46	1.71	0.60	0.9918	0.12	0.73	0.18
Exponential Cosine	0.9544	1.95	10.47	2.85	0.9282	0.71	4.29	1.06

Table 4.9, which is Filter Set 1 in Table 4.8, are smaller for the trimming with respect to the mean square ΔE_{Lab} error than they are for the trimming with respect to the measure. This is as expected, and illustrates the advantage of trimming with respect to the ΔE_{Lab} error.

4.6 Projection Methods

Projection methods have become popular ways of solving constrained optimization problems. Set-theoretic problem formulation allows the use of a wide range of constraints which is not possible using classical methods. A set-theoretic formulation of the problem of the design of colour scanning filters involves the definition of the following sets in the space of all Nxr matrices

The set of all filter sets of 'high enough' measure:

$$C_\nu \;=\; \{\mathbf{M}|\nu(\mathbf{A}_L, \mathbf{M}_H) \;\geq\; 1-\delta\}$$

and the set of filter sets with smooth filters:

$C_s \;=$

$$\{\mathbf{M} \;=\; [\mathbf{m}_1, ...\mathbf{m}_r]|\mathbf{m}_i(j+1) \;+\; \mathbf{m}_i(j-1) \;-\; 2\mathbf{m}_i(j) \leq \delta; 1 \leq i \leq r; 2 \leq j \leq N-1\}$$

The required solution is a filter set with high enough measure and consisting of smooth individual filters. Hence, the required solution lies in the intersection of the two constraint sets, and $\mathbf{M} \in C_\nu \cap C_s$ The set C_s is convex. On the other hand, the set C_ν is not. A simple example demonstrates this. Suppose $\mathbf{M} \in C_\nu$. This implies that $-\mathbf{M} \in C_\nu$, but $0.5(\mathbf{M} + -\mathbf{M}) = \mathbf{0} \notin C_\nu$ This implies that using set-theoretic methods to solve the problem will require the use of results from the theory of sequential projections onto non-convex sets. The implementation of sequential projections onto non-convex sets is beyond the scope of this dissertation. As the problem has been solved using simpler methods in the preceding section, it is not necessary.

4.7 Conclusions

The measure of goodness of a set of colour filters developed in Chapter 3 may be used to define an optimization criterion for a scanning system. The modelling of the filters as known, smooth, non-negative functions like the gaussian results in a parametrization of the filter design problem. The problem is framed as a simple optimization problem with respect to the parameters of the filter model. This problem may be satisfactorily solved by standard minimization (or maximization) routines to give filters with fairly high measures. Experimental results for two particular scanning characteristics are presented. Hardware implementation indicates that this method is very useful for designing filters for colorimetric applications. The gradient of the average square ΔE_{Lab} error may be used to trim the optimal solutions to significantly improve the parametrized solutions to produce smooth filters with low ΔE_{Lab} errors.